Tropical Water Quality Hub

National Environmental Science Programme

Final Report

Oceanographic drivers of bleaching in the GBR: from observations to prediction

Volume 2: 3D Bleaching in the GBR: Development and analysis of a 3D climatology and heat accumulation products using eReefs

Clothilde E. Langlais, Mike Herzfeld, Eduardo Klein, Neil Cantin,
Jessica Benthuysen and Craig Steinberg

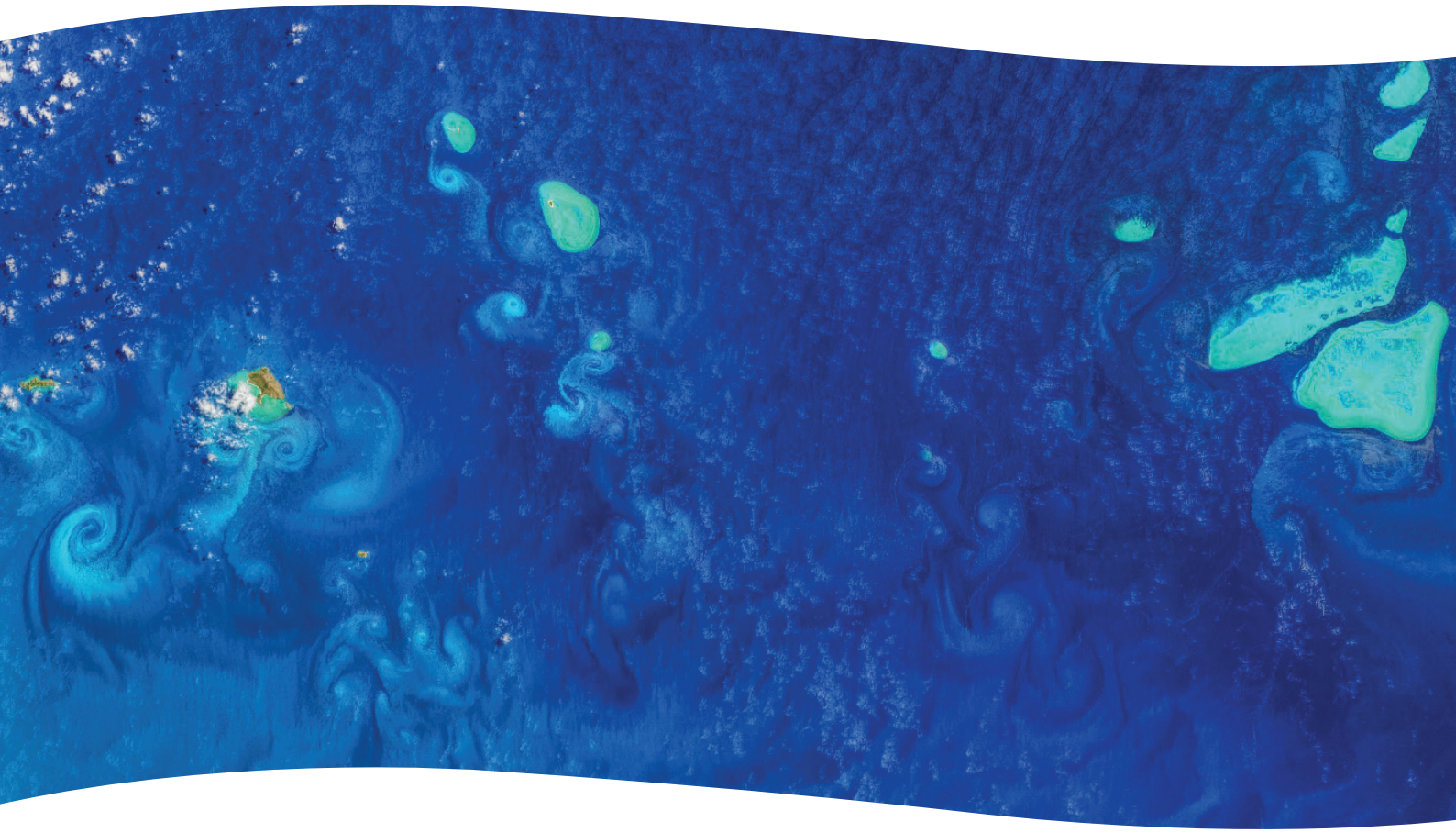

Australian Government

Australian Institute of Marine Science

Oceanographic drivers of bleaching in the GBR: from observations to prediction

Volume 2: 3D Bleaching in the GBR: Development and analysis of a 3D climatology and heat accumulation products using eReefs

Clothilde E. Langlais[1], Mike Herzfeld[1], Eduardo Klein[2], Neil Cantin[2], Jessica Benthuysen[3] and Craig Steinberg[2]

[1] CSIRO Oceans & Atmosphere, Hobart
[2] Australian Institute of Marine Science, Townsville
[3] Australian Institute of Marine Science, Crawley

Australian Government

National Environmental Science Programme

Supported by the Australian Government's
National Environmental Science Program
Project 4.2 Oceanographic drivers of bleaching in the GBR: from observations to prediction

National Library of Australia Cataloguing-in-Publication entry:
978-1-925514-89-6

This report should be cited as:
Langlais, C. E., Herzfeld, M., Klein, E., Cantin, N., Benthuysen, J. and Steinberg, C. (2021) *Oceanographic drivers of bleaching in the GBR: from observations to prediction, Volume 2: 3D Bleaching in the GBR: Development and analysis of a 3D climatology and 3D heat accumulation bleaching products using eReefs*. Report to the National Environmental Science Program. Reef and Rainforest Research Centre Limited, Cairns (55 pp.).

Published by the Reef and Rainforest Research Centre on behalf of the Australian Government's National Environmental Science Program (NESP) Tropical Water Quality (TWQ) Hub.

The Tropical Water Quality Hub is part of the Australian Government's National Environmental Science Program and is administered by the Reef and Rainforest Research Centre Limited (RRRC). The NESP TWQ Hub addresses water quality and coastal management in the World Heritage listed Great Barrier Reef, its catchments and other tropical waters, through the generation and transfer of world-class research and shared knowledge.

Cover photographs: (front) Fine scale circulation features around reefs in the GBR lagoon near the Pompeys Reefs. Landsat 8 Image, 27 October 2019; Image: NASA. (back) Bleached coral, John Brewer Reef; Image: Neal Cantin, AIMS.

This report is available for download from the NESP Tropical Water Quality Hub website:
http://www.nesptropical.edu.au

CONTENTS

LIST OF TABLES

LIST OF FIGURES

ACRONYMS

3D …….... three-dimensional
AVHRR ..... Advanced Very-High Resolution Radiometer
BGC..... BioGeoChemical
CC..... correlation coefficient
DHW ……. Degree Heating Week
DHW_SSTAARS…. 3D bleaching metrics using MMM_SSTAARS and GBR1
DHW_NOAA…… 3D bleaching metrics using MMM_NOAA and GBR1
DHW_CRW……..... NOAA's Coral Reef Watch DHW derived from satellite SST.
DHWmax ……. maximum value of DHW reached over the summer.
EAC ..... East Australian Current
GBR..... Great Barrier Reef
GBR1 ……..3D hydrodynamic,1 km resolution eReefs model
MMM …… Summer monthly maximum mean
MMM_NOAA…….. 3D NOAA-GBR1 MMM
MMM_SSTAARS….3D SSTAARS-GBR1 MMM
MSE ..... Mean squared error
NCI..... National Computing Infrastructure
NESP ..... National Environmental Science Program
NOAA ..... National Oceanographic and Atmosphere Administration
NRMSE ..... Normalized root mean square error
PBIAS..... Percentage Bias
SST ……. Sea Surface Temperature
SSTAARS ……The 2 km SST Atlas of the Australian Regional Seas
THREDDS..... Thematic Realtime Environmental Distributed Data Services
TWQ..... Tropical Water Quality

ABBREVIATIONS

˚**C** ..... degrees Celsius
˚**S** ..... degrees South
et al..... and others
km..... kilometre
m..... metre
N ..... number of samples
%..... percent

ACKNOWLEDGEMENTS

This research was supported by funding from the Australian Government's National Environmental Science Program (NESP) Tropical Water Quality (TWQ) Hub Project 4.2. The eReefs model simulations were produced as part of the eReefs project (eReefs.info), a collaboration between the Science Industry Endowment Fund (SIEF), the Commonwealth Scientific Industrial Research Organisation (CSIRO), the Australian Institute of Marine Science (AIMS), the Bureau of Meteorology (BOM), and the Great Barrier Reef Foundation (GBRF), with support from BHP Billiton Mitsubishi Alliance, the Australian and Queensland governments, and with observations obtained through the Integrated Marine Observing System (IMOS). The Sea Surface Temperature Atlas of the Australian Regional Seas was accessed through IMOS. In situ temperature data was provided by the AIMS weather station and temperature logger programs and the IMOS Queensland and Northern Australian Mooring sub-facility of the Australian National Mooring Network. IMOS is enabled by the National Collaborative Research Infrastructure strategy (NCRIS). It is operated by a consortium of institutions as an unincorporated joint venture, with the University of Tasmania as Lead Agent. All of NOAA Coral Reef Watch's products were accessed through a web portal at http://coralreefwatch.noaa.gov. NOAA Coral Reef Watch work is supported primarily by the NOAA Coral Reef Conservation Program and the NOAA National Environmental Satellite, Data, and Information Service's Center for Satellite Applications and Research.

PREFACE

For the first time, back-to-back mass coral bleaching occurred on the Great Barrier Reef (GBR) and Torres Strait in 2016 and 2017 as part of a continuous global bleaching event that started in late 2014 (Eakin et al, 2018). The combined effect has meant that the majority of the reef has been severely affected; however, there remain significant areas that have survived along the length of the GBR. This project seeks to understand how reef scale, regional and global oceanographic and meteorological processes influence the severity and spatial variability of thermally driven coral bleaching for the Great Barrier Reef and Torres Strait.

The project gathers available observations and uses them to assess and validate a range of model types from nowcasting and short-term forecasting eReefs models; sub-seasonal to seasonal predictive ACCESS models and the identification of regions and oceanographic mechanisms associated with them that produce persistent resistance to warming and coral bleaching through the development of a hazard map and an analysis of the eReefs model over mass coral bleaching events.

The report is structured in four main components with each written as separate volumes:

Volume 1 - Summary of oceanographic conditions during the 2015-17 bleaching years.

All available, relevant environmental observations of the recent bleaching events will be gathered to be more easily discoverable to researchers and managers via a gateway/summary webpage. These include hundreds of temperature loggers deployed along the GBR by AIMS, weather stations and the use of IMOS remote sensing, moorings and glider deployments. This publicly available and quality controlled data set will allow the most comprehensive understanding yet of how individual coral reefs faired in these events.

Volume 2 - 3D-Bleaching in the GBR: Development and analysis of a 3D climatology and heat accumulation bleaching products using eReefs.

The new eReefs 3D modelled heat accumulative bleaching products developed here provide a deeper understanding of bleaching refugia in the GBR. The algorithm is adapted from NOAA's widely used and globally recognised Degree Heat Week (DHW) satellite derived product. A common characteristic of proposed refugia is a reduction in temperature variability and a certain insensibility to extreme conditions. We show that the understanding of regional oceanographic processes is key to understand the effectiveness of cool water persistence that can counteract warming processes and the heat stress that leads to coral bleaching. New heat accumulative bleaching products were developed, blending a climatology of high-resolution SST observations (The 2-km Sea Surface Temperature Atlas of the Australian Regional Seas; SSTAARS) with a high-resolution 3D hydrodynamic model, the 1km eReefs model (GBR1).

Volume 3 – Development of a hazard map for the Great Barrier Reef to predict regions with a lower risk of persistent warming and coral bleaching.

A hazard map is a framework for risk assessment consisting of a series of geographical layers or maps that defines:

a) The location of static conditions that may induce or reduce the incidence of bleaching in coral communities. These layers include the detailed bathymetry and derived characteristics, like the steepness of the reefs front and the presence of inter-reef channels;
b) The climatology of some oceanographic and meteorological variables that are known to be a factor that could induce or protect the corals from bleaching, like accumulated heat, recurrent upwelling areas, tidal mixing areas, photosynthetically active radiation (PAR) and the probability of mixing of the water column; and
c) The anomaly maps for each of the analysed variables for 2016 and 2017 related to its climatology. This report presents the climatology and the corresponding anomalies of oceanographic and meteorological variables that may promote or protect coral reef from bleaching. The potential of a predictive capability using this technique is also explored.

Volume 4 – Observations and predictions of marine heatwaves in the GBR

Development of skilful marine heatwave prediction tools are critical for marine management of ecosystem resources and services. This project aims to synthesise our knowledge of marine heatwaves (MHW) over the GBR Marine Park (GBRMP) and adjacent Coral Sea and investigate ways to apply state-of-the-art ocean prediction systems for MHW predictions. First, we applied a recently developed marine heatwave framework to consistently quantify marine heatwave metrics over the GBR and Coral Sea using a sea surface temperature product. We found that mass coral bleaching events in the GBR coincided with some of the longest, most spatially extensive, and severe MHWs during summer months in the satellite record. We then used these results to explore ways in which sub-seasonal to seasonal prediction systems can be used for MHW prediction. We provide recommendations on further areas of research and how users can interpret predictions from short-term (10 days) to seasonal (months) time scales in the context of MHWs. This study is timely given the extensive 2020 MHW and mass coral bleaching along the GBRMP and Coral Sea.

EXECUTIVE SUMMARY

After three mass coral bleaching events in the last five years, strategies to protect the Great Barrier Reef (GBR) have never been so timely and critical. Historically, the 1998, 2002 and 2016 mass coral bleaching in the GBR have been associated with the positive phase of ENSO. However, in recent years, mass coral bleaching events in 2017 and 2020 occurred while ENSO was neutral. As the climate continues to warm, the positive phase of the climate mode is no longer a necessary condition for bleaching risk in the GBR, and the number of potential reefs refugia is declining (Hughes et al., 2017). The question is whether there remain regions that are insensitive to climate variability and change, i.e., low variability areas that could act as refugia.

Identifying and protecting spatial refugia is a common strategy for coral reef conservation (West et al., 2003; Beyer et al., 2018). The challenges in determining which part of the GBR could potentially be refugia are multiple:

- Geographic bleaching footprints vary from year to year, depending on the development of the marine heatwaves. While marine heatwaves can be reinforced by weakened monsoon, reduced cloud cover or increased heat transport by currents, local or regional weather events and ocean processes may lead to a temperature reduction and, hence, protect reefs from heat stress and bleaching.
- Because of the size of the GBR, in-situ observations of mass coral bleaching are scattered and intermittent. In 2016 and 2017, comprehensive diver surveys in the top 10m of the water column only covered between 50-60% reef area of the GBR. Observations at the scale of the GBR can only be made from aerial surveys or satellite remote sensing.
- Operational bleaching algorithms such as ReefTemp Next Generation and NOAA's Coral Reef Watch Degree Heating Week (DHW) bleaching products are derived from remotely sensed Sea Surface Temperature (SST) products, making the use of operational bleaching product rely upon the assumption that surface temperature anomalies also apply at depth.
- The 2km spatial resolution of ReefTemp and 5km spatial resolution of the NOAA satellite-based product cannot fully capture the reef scale response to meso and sub-mesoscale processes like upwelling, filaments, eddies, and internal tides and waves.

These limitations have prompted us to use the eReefs hydrodynamical model to map the spatial footprint of bleaching events at 1km resolution, as well as the depth to which heat stress penetrates. This is critical to identify regions where corals may escape bleaching: surface refugia but also deeper slopes or lagoons, even though those nearer to the surface will be subject to bleaching. New heat accumulative bleaching products (DHW products) were developed, blending high resolution SST climatology from observations (The 2km Sea Surface Temperature Atlas of the Australian Regional Seas; SSTAARS) with high resolution 3D hydrodynamical model, the 1km eReefs model (GBR1).

The DHW products

The development of 3D bleaching products requires not only 3D temperature timeseries, but also a 3D climatology. Indeed, it is important to adjust the thermal threshold to conditions experienced at depth.

As the 5-y GBR1 archive is too short to calculate a climatology, we created a 3D version of the thermal thresholds, by combining a surface observational climatology (SSTAARS) with the GBR1 temperature profiles scaled with surface values.

To directly compare our eReefs DHW products with the NOAA's Coral Reef Watch DHW product, we also combine the NOAA's Coral Reef Watch MMM with the scaled GBR1 temperature profiles, to create a second thermal threshold.

To maintain consistent interpretation of derived bleaching products, our DHW product mirrors some characteristics of the NOAA's Coral Reef Watch DHW product. First, we use daily snapshot of temperature at night from GBR1 for the calculation of 3D temperature anomalies. Secondly, we re-centred the SSTAARS climatology two decades earlier, in order to obtain a thermal threshold comparable in amplitude with the NOAA's threshold.

Overall, this study shows that using SSTAARS climatology centred in 1985 and GBR1 modelled daily night temperature, provides an accurate DHW product, comparable with the Coral Reef Watch product at regional scales and at the surface, with the advantages of adding details to the spatial footprint of bleaching as well as resolution at depth.

3D bleaching in the GBR

The new DHW products provide a deeper understanding of bleaching refugia in the GBR. A common characteristic of proposed refugia is a reduction in temperature variability and a certain insensibility to extreme conditions. We show that the understanding of regional oceanographic processes is key to understand the effectiveness of cool water persistence that can counteract warming processes and the heat stress that leads to coral bleaching.

We show that upwelling areas in the GBR have been consistently acting as a barrier to bleaching during the past three mass coral bleaching events. In the past five years, we found that the only area that stayed below 4°C-week at the surface is the southern outer reef which is protected by the current-induced upwelling and the strong regional tides allowing the cooler waters to mix to the surface. In the far north GBR and eastern Torres Strait, the tide-induced mixing tends to reduce heat stress throughout the water column. In the Central GBR, the upwellings do not reach the surface, but the sub-surface cooling has the capacity to protect areas below 24m.

The East Australian Current plays a double game here: it is a medium for extra heat as well as a trigger of upwellings. The EAC carries extra heat resulting in a ribbon of high risk along the shelf break. But it also protects the reef because the association of thermocline uplift and tidal mixing mixes cooler waters to the surface and channels them onto the continental shelf between the outer ribbon reefs, providing a ribbon of persistent tidally modulated cooling.

A consequence is that zones of high and low bleaching risk are adjacent to each other along the shelf break.

These sharp spatial gradients are not reproduced by the 5km resolution Coral Reef Watch products, which only show bleaching patterns with smoothed spatial variations, limiting the ability to identify refugia. Comparison of our results with bleaching aerial surveys shows consistency between our identified surface refugia and areas that consecutively experienced low bleaching in 2016 and 2017.

1.0 INTRODUCTION

1.1 Great Barrier Reef under the threat of heat-driven mass bleaching events

The Great Barrier Reef (GBR) is the world's largest reef structure (Figure 1), supporting diverse ecosystems and providing critically important ecological and social services. To protect the GBR, conservation management systems need to account for multiple stressors: reef damage from tropical cyclones, Crown of Thorns Starfish outbreaks, declining water quality from terrestrial nutrient and sediment input, ocean acidification, marine heatwaves and coral bleaching. However, in recent years, the reef resilience and its capacity to adapt have been overwhelmingly challenged by one particular stressor: severe heat stress, with significant attention given to heat-driven mass bleaching events (Hughes, 2017).

Coral bleaching occurs when reef-building corals expel their dinoflagellate symbiont, zooxanthellae, due to external stressors (Glynn, 1996). Without the photosynthetic products provided by the symbiont, many essential physiological processes such as calcification and reproduction, are suppressed. Over extended periods of time as short as six weeks, the loss of zooxanthellae can ultimately lead to coral death (Jones, 2008). Coral bleaching can be driven by a range of stressors from heat stress to freshwater flood plumes or pollution, with multiple stressors being more detrimental for coral reefs. However, the mass bleaching events in recent decades have been driven by prolonged global marine heatwaves exacerbated by climate change and are extremely detrimental to coral reef health and recovery (Hoegh-Guldberg, 1999; IPCC, 2019).

A primary aspect of climate change is ocean warming which has major impacts throughout the world's oceans. In particular, mass coral bleaching events have increased in frequency over the past two decades due to warming, resulting in reef degradation worldwide (IPCC, 2019). The exposure of the GBR to mass bleaching events is becoming more recurrent, with events recorded in 1998, 2002, 2006, 2016, 2017 and 2020. The 2016-2017 severe and widespread coral bleaching event impacted more than 70% of the world's coral reefs (Heron et al., 2017), leading to mortality and a decrease in coral cover. The gravity of the record-breaking marine heatwave was reinforced by the prolonged nature of the rolling mass bleaching event which impacted worldwide reefs in three consecutive years 2014-2017 (Eakin, 2018) and for the first-time back-to-back bleaching in 2016 and 2017. In the GBR," *At the end of the back-to-back bleaching event of 2016-2017, 45% of the total reef area was exposed to extreme heat stress (DHW > 8), with reefs at this level of heat stress resulting in 51% of the coral community (median) dead or dying (Bleaching State 5+6, severely bleached)"* (from Cantin et al. 2020).

1.2 Reef management

After three mass coral bleaching events in the last five years, strategies to protect the GBR have never been so timely and critical. Marine protected areas, fisheries management and improvements in water quality are all important aspects of reef management.

But after the longest (2014-2017), most widespread and most damaging global bleaching event ever recorded (Hughes et al., 2018), it is becoming clear that CO_2 emission reduction in combination with reef resilience assessment and support to reef recovery is the key to save the reef (McLeod et al., 2021). Identifying and protecting spatial refugia is a common strategy for coral reef conservation (West et al., 2003; Beyer et al., 2018), but the number of potential reefs refugia is declining (Hughes et al., 2017).

1.3 Tracking coral bleaching

Optimal coral growth occurs at just a few degrees below the thermal limit of the symbiosis between the coral host and the zooxanthellae (Marshall and Code, 2004). Above this limit, the photosynthetic processes break down, resulting in accumulation of toxic reactive oxygen that is harmful for the coral host. If the exposure lasts for too long, the expulsion of the symbiont becomes the only protective mechanism for the host (Fitt et al. 2001). This physiological reaction explains why thermal stress and coral bleaching have been empirically related to the accumulation of temperature anomalies above a “thermal threshold” (Glynn et al., 1990, Berkelmans et al., 1999). It is not only the amplitude of the temperature anomaly but also the period of exposure to that anomaly that leads to coral bleaching conditions.

Cumulative heat stress metrics (see Donner (2011) for a review) are widely used with near real-time satellite monitoring (Liu et al, 2014) and future projections (vanHooidonk et al. 2013; Langlais et al., 2016). Operational bleaching algorithms such as ReefTemp Next Generation (http://www.bom.gov.au/environment/activities/reeftemp/reeftemp.shtml) and NOAA’s Coral Reef Watch (https://coralreefwatch.noaa.gov/) bleaching products are derived from remotely sensed sea surface temperature (SST) products. Both SST anomalies and thermal thresholds are derived from remotely sensed SST products, limiting the interpretation of what is happening at depth. To get to the scale of individual reefs, higher resolution is also needed. The 5km spatial resolution of the Coral Reef Watch product cannot fully capture the reef scale response to meso and sub-mesoscale processes like upwelling, filaments, eddies, and internal tides and waves.

Here we propose to implement high-resolution, 3-dimensional (3D), depth-resolved equivalents of the bleaching products, using numerical models to retrieve temperature profiles. This is critical to understand the spatial footprint of bleaching as well as the depth to which thermal stress occurs and identify regions where corals may escape bleaching: surface refugia but also deeper slopes or lagoons that may escape bleaching even though those nearer to the surface will be subject to bleaching. Oceanographic circulation features may affect thermal stratification of the water column, in particular during the Monsoon season (Figure 1). During the Monsoon season, uplifted cold water mass can maintain cold conditions throughout the water column.

Venegas et al. (2020) stressed how important it is to adjust the thermal threshold to depth conditions. The development of 3D bleaching products requires a 3D climatology and 3D temperature timeseries.

While there are a number of climatologies developed for SST, there are fewer climatologies available accounting for temperature variations with depth. In the GBR, the CSIRO Climatology of Regional Seas (CARS, http://www.marine.csiro.au/~dunn/cars2009/) (Ridgway et al. 2002) and the Australia Shelf Seas Atlas (https://www.wamsi.org.au/news/new-shelf-seas-atlas-australia) are the only 3D observations-based climatologies. While CARS climatology has a 0.5° horizontal resolution and 79 vertical levels varying between 0 and 5m from 0 to 300m, the Atlas has a higher horizontal resolution of 0.25°, but a lower vertical resolution with 10m depth intervals from surface to 500m.

Combining high-resolution observations and modelling outputs is the best way to obtain a 3D climatology in the GBR. Here, we propose to blend high resolution SST observations (The 2km Sea Surface Temperature Atlas of the Australian Regional Seas; SSTAARS) with high resolution 3D hydrodynamical model, the 1km eReefs model (GBR1).

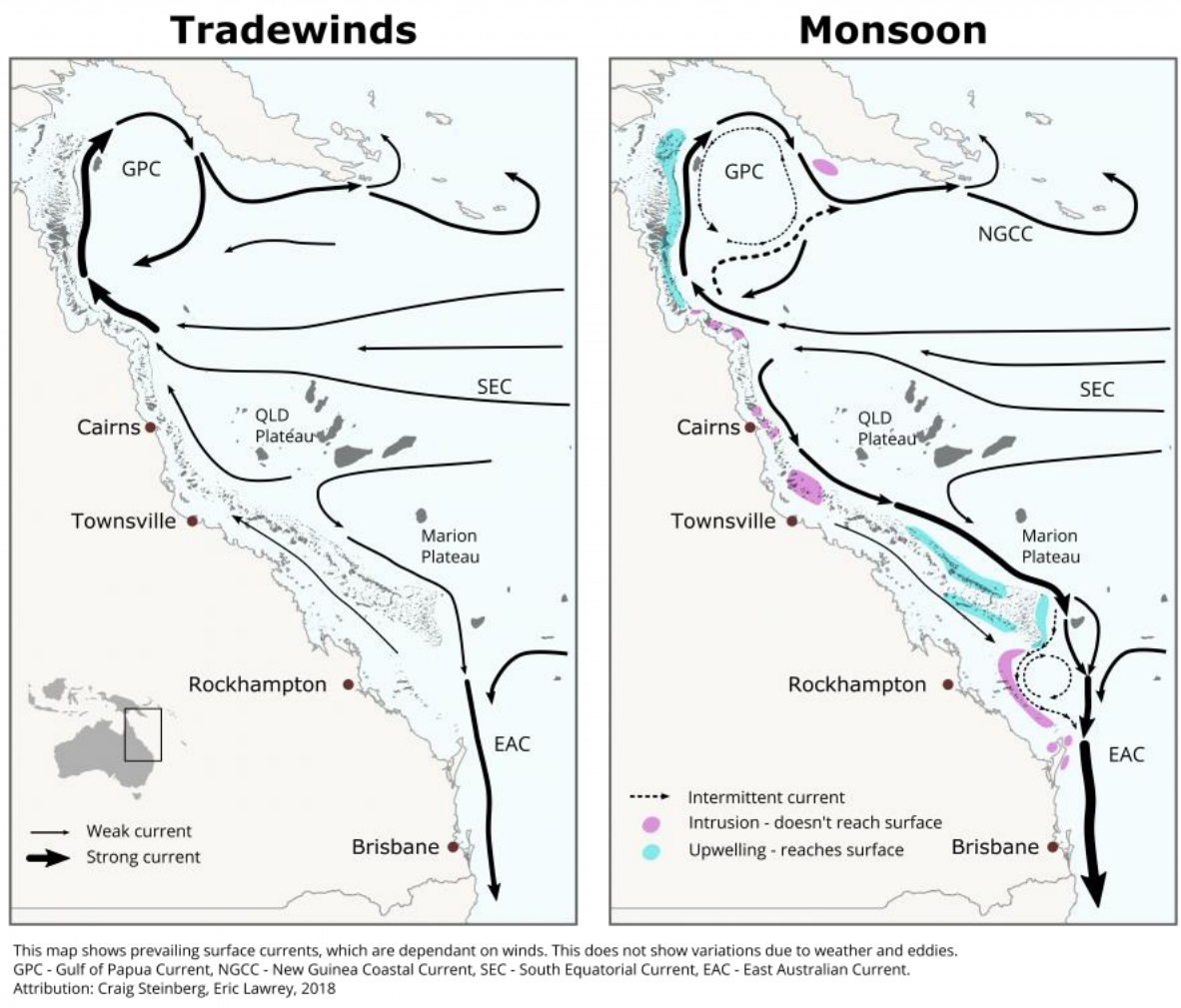

Figure 1: Prevailing surface currents

2.0 METHODOLOGY

2.1 Degree Heating Week bleaching metric

Coral bleaching risk has been empirically related to the accumulation of SST anomalies above a “thermal threshold” (Glynn et al. 1990; Berkelmans et al., 1999). The most commonly used bleaching risk metric, Degree Heating Week (DHW) (Liu et al., 2003), defines the thermal threshold as 1°C above the warmest monthly typical conditions from the climatology, defined as the monthly maximum mean (MMM). The MMM can be thought of as the optimal temperature for coral growth, while the +1°C threshold accounts for a level of initiating stress to the higher-than-normal warm season temperatures (Berkelmans et al., 1999).

DHW is defined as the accumulation of hotspots (SST anomalies relative to MMM) over the past 12-week window when SST is warmer than the thermal threshold (MMM+1°C) (Liu et al. 2003). In other words, only hotspots larger than 1°C, are accumulated over the past 12-week window which slides one day at a time. This accumulation results in a daily DHW product which is reported in temperature anomalies per week (°C-weeks): the 12-week accumulated anomalies are divided by 12. Coral Reef Watch has an online tutorial explaining step by step how their 5km DHW product is calculated:
(https://coralreefwatch.noaa.gov/product/5km/tutorial/welcome.php) (Figure 2).

Coral Reef Watch currently uses data from eight satellites operated by NOAA and partners to produce a daily measurement of the night-time ocean temperature at the sea surface, calibrated to 0.2 metres depth (Skirving et al., 2020). This daily SST product is then used to build the daily global 5km satellite coral bleaching DHW product.

Empirical evidence suggests that significant coral bleaching usually occurs when the DHW value reaches 4°C-weeks, and severe and widespread bleaching occurs when DHW is greater than 8°C-weeks (Liu et al., 2003, Eakin et al., 2010). Above this limit, there is a high risk of coral mortality, lower rates of growth, calcification and reproduction, and larval recruitment (Baker et al. 2008).

To compare the spatial and depth footprint of bleaching risk between different years and different DHW products, we calculate the maximum value of DHW reached over each summer (DHWmax). The development of 3D bleaching products requires a 3D MMM and 3D daily temperature hotspots.

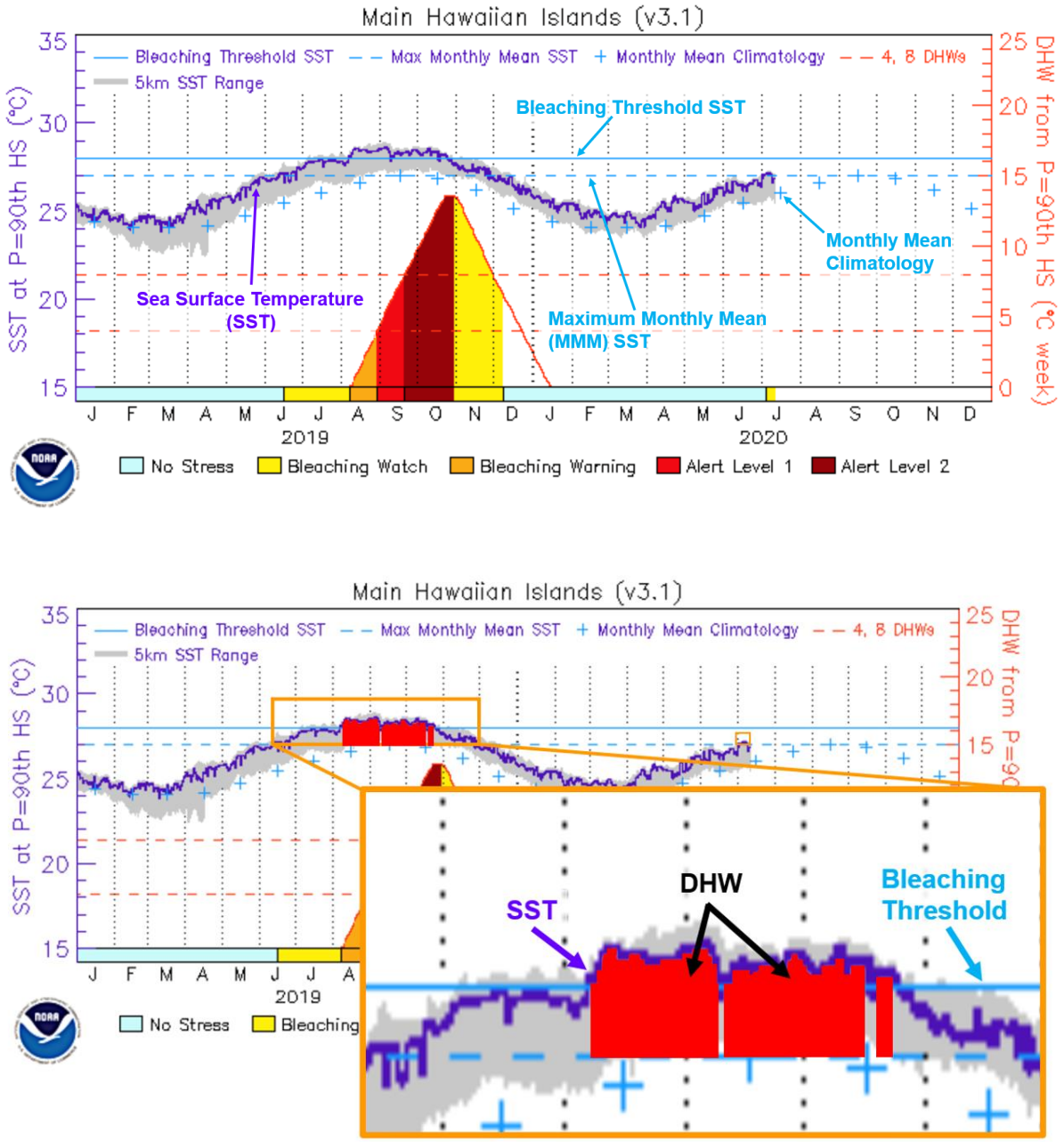

Figure 2: DHW calculation example at the Main Hawaiian Island virtual station: SST and DHW timeseries alongside all the different thresholds, monthly maximum mean (MMM), thermal threshold (MMM + 1°C), 4°C-weeks bleaching limit and 4°C-weeks severe bleaching limit (top), zoom over the period when SST is above the thermal threshold, hotspots larger than 1°C are highlighted in red (bottom).

Source: https://coralreefwatch.noaa.gov/product/5km/tutorial/crw10a_dhw_product.php

2.2 3D Degree Heating Week product

To build a 3D DHW product, we blended the 2km SST observations SSTAARS with the 1km GBR1 3D hydrodynamical model. After a short description of these two products, this section describes how the SST climatology is extended at depth by incorporating the vertical temperature structure produced by GBR1 and how the 3D MMM is generated.

2.2.1 SSTAARS

For coastal water surrounding Australia, the most recent high-resolution product available is the Sea Surface Temperature Atlas of the Australian Regional Seas (SSTAARS) (Wijffels et al., 2018). The product is based on 25 years (1992-2016) of Advanced Very-High Resolution Radiometer (AVHRR) for night-time only SST and is at approximately 2km horizontal resolution (Figure 3 left). The climatology is based on sinusoidal fits and a linear trend to the data (Wijffels et al., 2018). The daily climatology fit is available from the Australian Ocean Data Network (AODN) Portal (https://portal.aodn.org.au/search).

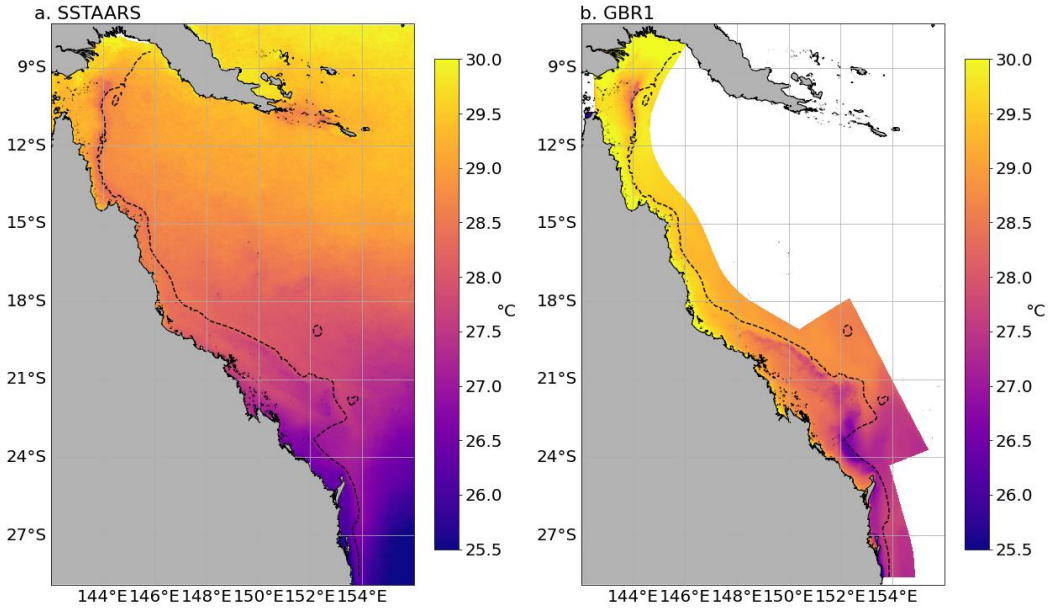

Figure 3: Sea Surface Temperature in the GBR - March climatology: 25-year (1992-2016) SSTAARS climatology (a.), 2015-2019 GBR1 climatology (b.), the black dashed line is the 200m isobath.

2.2.2 eReefs model

The eReefs research project (https://ereefs.org.au/ereefs) is a collaboration between the Great Barrier Reef Foundation, CSIRO, the Australian Institute of Marine Science (AIMS), Bureau of Meteorology, and Queensland Government. A component of the project is the development of an information platform that provides a picture of what is currently happening on the reef and what will likely happen in the future (Steven et al., 2019). As stated in Steven et al. (2019), eReefs products *"inform operational activities, enable reporting of marine water quality and have also been used for scenario planning to address a number of issues confronting the GBR including: the setting of catchment nutrient and sediment targets, reporting on the environmental condition of and outlook for the GBR, prediction of coral bleaching and the*

testing of potential geo-engineering and adaptation approaches, ocean acidification vulnerability, and the occurrence and spread of the crown-of-thorns starfish."
The eReefs hydrodynamic models are available at 4km (GBR4) and 1km (GBR1) horizontal resolution. Both models have the same vertical resolution, with 47 layers and 1m resolution near the surface.

The latest version, v2.0, is available from Oct 2010 – present for GBR4 and Dec 2014 – present for GBR1. GBR4 and GBR1 are operating routinely in near real-time within the CSIRO real-time framework. These model outputs are routinely posted on the web (https://research.csiro.au/ereefs/models/modeloutputs/), and are publicly available through the NCI THREDDS server (http://dapds00.nci.org.au/thredds/catalogs/fx3/catalog.html). A six-year archive currently exists of the 1km output, which is appended using the routine near real-time output (Figure 3). These models have been subject to calibration and validation, both in hindcast and near real-time, using available Reef Rescue monitoring data, data from AIMS and CSIRO cruises, data from the Integrated Marine Observing System and satellite observations (Herzfeld et al., 2016). Skill assessment indicates that the models are performing well at the surface for temperature in terms of the annual and weather band cycles. Surface salinity shows good agreement in the timing and magnitude of river flood events. Biases exist in temperature and salinity at depth, which are speculated to be due to initial and boundary conditions. Diurnal and low frequency sea level correlate well with observations (Herzfeld et al., 2016).

In this report, we extend the validation of GBR1 for the most recent years (2016-2020) using oceanographic observations from the 2016 & 2017 bleaching summers (from the first report volume of the NESP TWQ Hub Project 4.2) and satellite observations (see section 2.3 for details about the observations).

While this report only focusses on the hydrodynamic model, we use the coral reef locations from the BioGeoChemical (BGC) and sediment model version 3.2. In GBR1, 26,163 grid cells host some coral reefs biomass (Figure 4). The reef locations were identified using habitat maps from the Allen Coral Atlas (Roelfsema et al., 2020). The database contains around 50,000 shapes, accounting for approximately 3,000 reefs. Note that this does not account for reefs north of 10.7^{o}S which is outside of the GBR Marine Park.

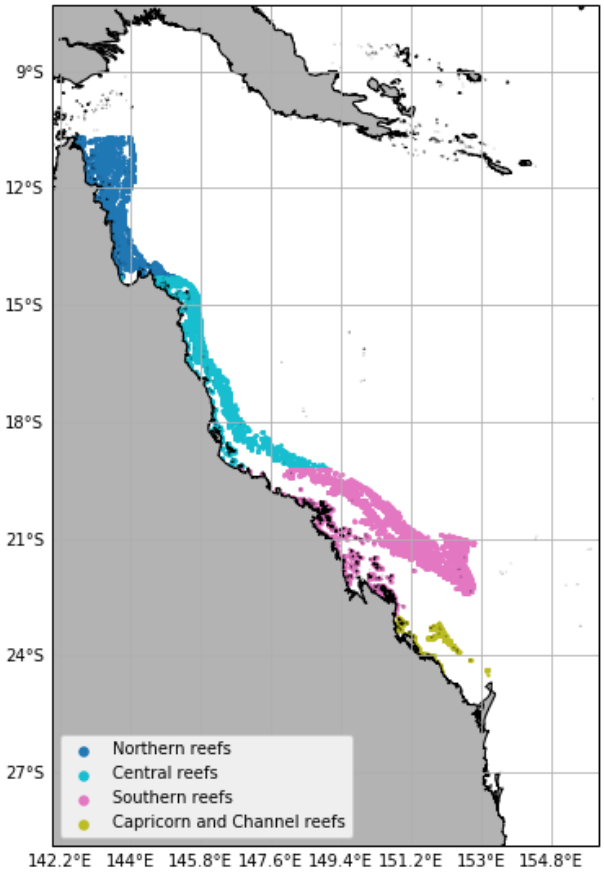

Figure 4: Coral reefs location in GBR1: grid cell hosting coral reefs identified using habitat maps from the Allen Coral Atlas (Roelfsema et al., 2020). The coloured dots show the individual reefs separated into different geographical zones.

2.2.3 eReefs GBR1 stratification and SSTAARS-GBR1 3D climatology

To extend SSTAARS at depth, we incorporated the vertical temperature structure produced by GBR1.

GBR1 scaled vertical profiles

We used the eReefs GBR1 output archive, produced by the version v2.0 of the hydrodynamical model (December 2014 to February 2019 at the time of calculation). We produced a climatology monthly mean temperature profile, based on five years for January and February and four years for March to December. For the profile calculation, GBR1 was re-run in "transport mode", where the outputs were sampled in 3D at 1hour intervals.

Each vertical temperature profile is a locally scaled profile with the surface as reference: $T_{p,}$ is simply the temperature at some depth, T_z, divided by the temperature at the surface, T_0; $T_p=T_z/T_0$. By dividing by the surface values, we obtain a profile of scaling values between 1-0. If the surface temperature is the same as that at depth then $T_p = 1$, and if cooler temperatures are found at depth the $T_p < 1$.

The scaled vertical profiles can then be used with any surface values to reconstruct a vertical temperature profile. Note that this profile is not a measure of climatology, rather a measure of stratification. If an anomalously warm year had its temperature increase uniformly distributed with depth, then there would be no change to the normalised profile.

Seasonal variations of the vertical profile climatology occur through changes to stratification, which reflect changes to net heat flux or freshwater inputs at seasonal scale. The season signal is larger than stratification changes due to inter-annual variability. As the five available summers of GBR1 is too short to create a daily temperature climatology, we produce a monthly mean profile over this period which incorporates N = (30 days x 5 years) = 150 days which is statistically more robust.

SSTAARS-GBR1 climatology

As the GBR1 archive is too short to calculate a climatology, we generate a 3D climatology by projecting the SSTAARS climatology throughout the water column using the spatially variable monthly scaled profiles.

The first step is to average the daily SSTAARS 2km climatology to create a monthly climatology with the same temporal resolution as the scaled vertical profile. The second step is to project the resulting monthly climatology onto the GBR1 grid on which the bleaching metrics will be later calculated. We then used the monthly scaled vertical profiles, to project the monthly surface climatology throughout the water column. The result is a 3D monthly climatology: 3D SSTAARS-GBR1 climatology. As noted above, it is important to keep in mind that the vertical structure is based on five years for January and February and four years for March to December, while the surface value has a (1992-2016) temporal reference. Table 1 summarizes the different products used for this study.

2.2.4 3D MMM and 3D DHW

3D MMM

To calculate 3D bleaching metrics on the GBR1 grid, we need a local climatological monthly maximum mean temperature for each grid cell and each depth. We created a 3D version of the MMM thermal thresholds, by combining surface observational products with the normalized GBR1 temperature profiles. We use two surface products: SSTAARS and the NOAA's Coral Reef Watch MMM. The first product provides the highest resolution for the region. The use of the second product allows us to directly compare our eReefs DHW products with the NOAA's Coral Reef Watch DHW product.

Using the 3D SSTAARS-GBR1 climatology, the monthly maximum values are selected for each grid cell and depth. For each grid cell, it is either January, February or March, and can vary from one depth to the other. The resulting 3D SSTAARS-GBR1 MMM (reference as MMM_SSTAARS) represents the warmest monthly conditions any grid cell can experience.

For the NOAA product, the procedure to calculate the 3D NOAA-GBR1 MMM (reference as MMM_NOAA) differs a little, as we directly use the MMM from Coral Reef Watch. For each grid cell at depth, the MMM_NOAA value is defined as the surface MMM multiplied by the normalized GBR1 profile value of the warmest month in the 3D SSTAARS-GBR1 climatology for that specific location. In effect, we use the month of the maximum temperature in the 3D SSTAARS-GBR1 climatology product to project the NOAA's Coral Reef Watch MMM at depth.

Adjusting the thermal threshold in time

The MMM_NOAA and MMM_SSTAARS are not centred on the same year. The latest NOAA MMM is based on a 28-year climatology (1985-2012) which was re-centred in 1988.3 using the linear trend of the summer months. Re-centring was necessary to maintain consistency with earlier versions of the NOAA products where the climatology was centred in 1987.5 (Heron et al., 2015). As SSTAARS is based on 25-year (1992-2016), centred in 2005, MMM_SSTAARS displays higher temperature than MMM_NOAA (Figure 5).

To maintain consistent interpretation of derived bleaching product, we use the SST trend from the SSTAARS climatology to re-centre the MMM_SSTAARS (Figure 5). As the SSTAARS trend is not seasonal but accounts for the timeseries, we re-centred SSTAARS with the objective to obtain comparable temperature range between MMM_NOAA and MMM_SSTAARS. In the following, we use the MMM_SSTAARS re-centred two decades earlier in 1985. Table 1 summarizes the different products used for this study.

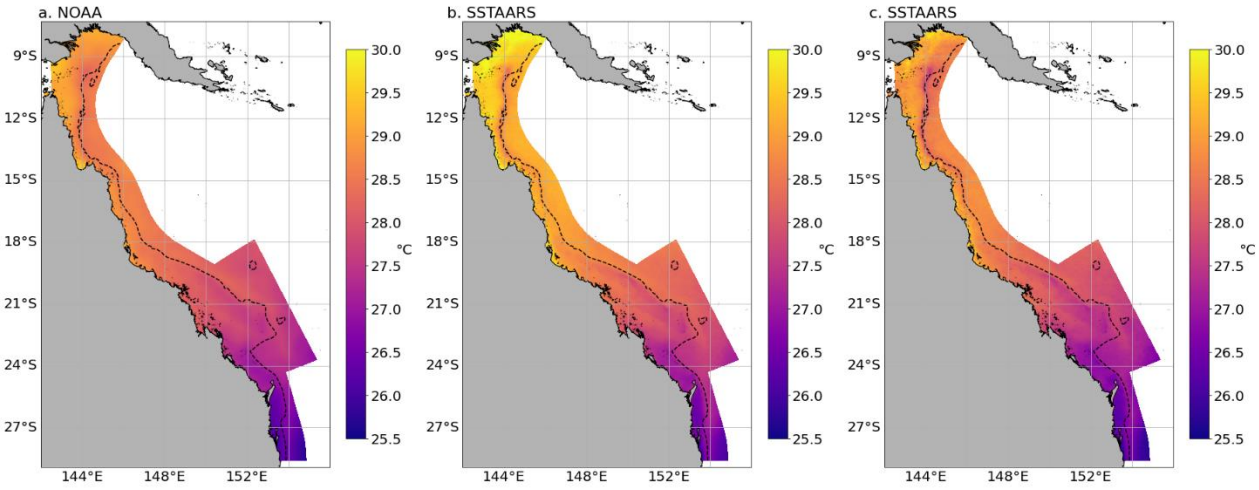

Figure 5: MMM maps: SST values from NOAA centred in 1987.3 (a.) and SST values from SSTAARS centred in 2005 (b.), and centred in 1985 (c.), the black dashed line is the 200m isobath.

3D DHW

Two eReefs DHW products are presented in this report. Both use the daily night-time snapshot 3D GBR1 temperatures for the 2016 to 2020 summers. 3D hotspots are calculated using two different 3D MMM: MMM_SSTAARS and MMM_NOAA. The 12-week accumulation results in two 3D DHW products, called DHW_SSTAARS and DHW_NOAA. Finally, maximum DHW values at each grid point are used to assess the maximum stress over each summer. At the surface, both products can be directly compared with the NOAA's Coral Reef Watch DHW product (referred as DHW_CRW). Table 1 summarizes the different products used for this study.

Table 1: Summary of the different climatology and bleaching products

Name	Spatial dimension	Spatial resolution	Temporal resolution	Time period	Climatology Central year	Re-centred	Data type
SSTAARS climatology	2 D	2 km	daily	1992-2016	2005	No	Observations
SSTAARS-GBR1climatology	3D	1km	monthly	1992-2016	2005	No	Observations and model
NOAA's Coral Reef Watch MMM	2D	5km	mean	1985-2012	1988.3	Yes	Observations
MMM_SSTAARS	3D	1km	mean	1992-2016	1985	Yes	Observations and model
MMM_NOAA	3D	1km	mean	1985-2012	1988.3	Yes	Observations and model
DHW_CRW	2D	5km	daily	1985-now	-	-	Observations
DHW_NOAA	3D	1km	daily	2015-now	-	-	Observations and model
DHW_SSTAARS	3D	1km	daily	2015-now	-	-	Observations and model

3.0 RESULTS

3.1 eReefs validation

3.1.1 Oceanographic observations

To validate the GBR1 temperature output we used a sample of temperature records from loggers that AIMS maintains across the GBR (http://data.aims.gov.au). For this particular validation we selected sites with data from summer months of 2016 and 2017 bleaching years at reefs that have had coral bleaching surveys. It resulted in a set of 103 sites with loggers at 236 locations at reef flat, reef slope or reef channel, ranging from one metre (reef flat) to 10 metres (reef slope and channel) depth (figure 6). The GBR1 hourly temperature series were extracted at each site at a matching depth by linearly interpolating from the values of the closest GBR1 depths. We also used temperature loggers from mooring arrays at six different sites from 10 to 190 metres depth and extracted the GBR1 time series in a similar way.

To evaluate the accuracy and precision of the GBR1 output, a set of indicator statistics were calculated:

- **Willmott**: Index of agreement between predicted and observed values. This metric compares the squared differences between the predicted (GBR1) and observed (loggers) values around the observed mean. It varies between 0 and 1. A value of 1 indicates a perfect match, and 0 indicates no agreement at all. (Willmott, 1981; Willmott et al., 2012).
- **pBias**: Percentage bias. Percent bias (PBIAS) measures the average tendency of the simulated values to be larger or smaller than their observed ones. The optimal value of PBIAS is 0.0, with low-magnitude values indicating accurate model simulation. Positive values indicate model overestimation bias, whereas negative values indicate model underestimation bias.
- **nrmse**: Normalized root mean square error (NRMSE) summarises the mean squared differences between predicted and observed values standardised by the standard deviation of the observed values.
- **mse**: Mean squared error. It is the mean of the squared differences between predicted and observed values.
- **cc**: Pearson correlation coefficient.

All the metrics were calculated using the R package HydroGOF (version 0.4-0, Zambrano-Bigiarini, 2020).

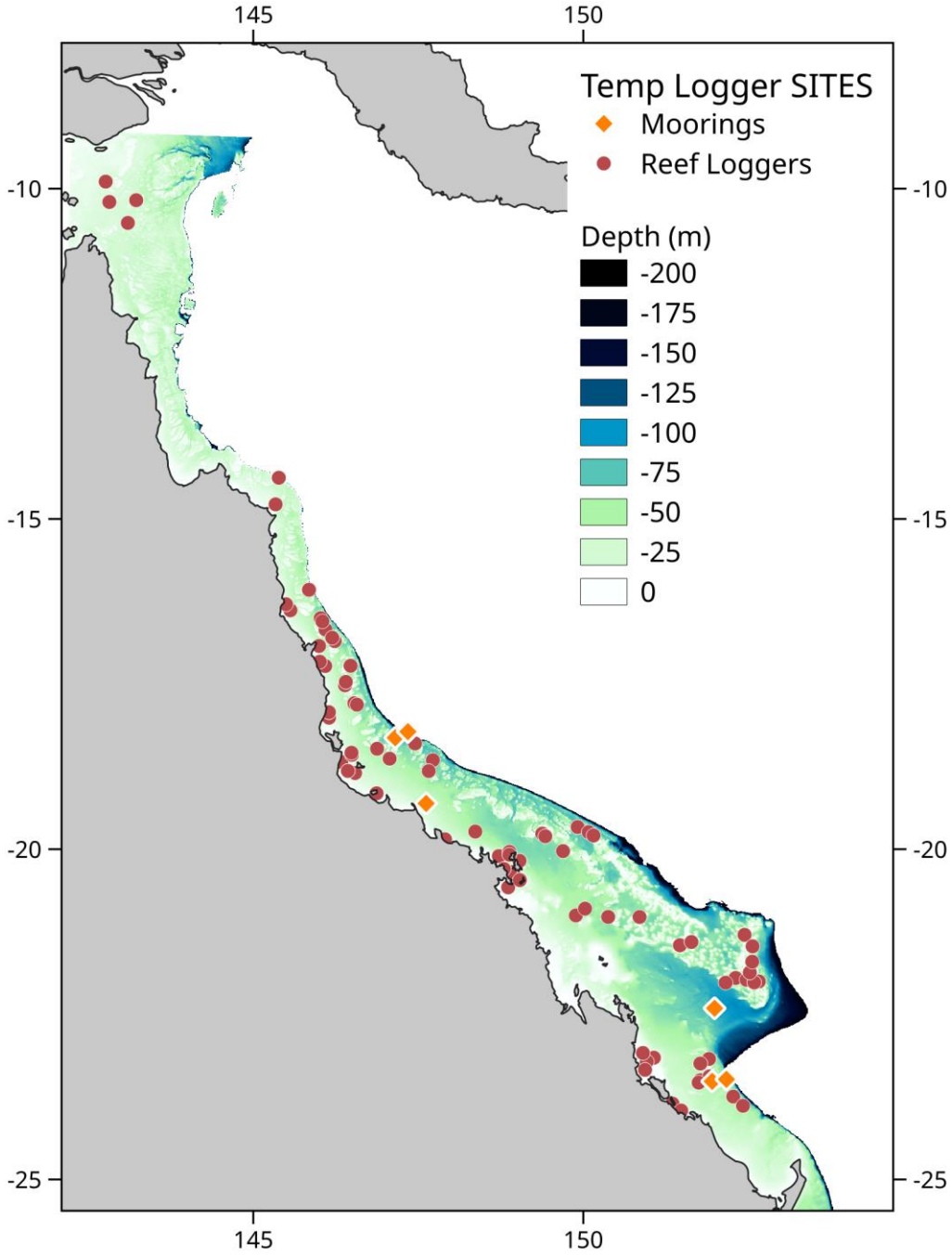

Figure 6: Temperature logger sites used for GBR1 validation. Bathymetry is from Beaman (2017) and depths are negative.

3.1.2 Model – observations comparison

For the summer months of 2016 and 2017, on average, the temperature from GBR1 was 0.32°C warmer than the reef temp loggers and 0.32°C cooler than the moored temperature loggers especially at deep locations (Table 2). 75% of all differences fall between 0.38°C and 0.73°C around the mean difference for reef locations and mooring locations respectively (figure 7). Detailed statistics for all sites are presented in the Appendix 1.

Table 2: Summary of GBR1 vs. temperature logger validation at mooring and reef sites for 2016-2017.

Source	Number of logger locations	Number of match ups in time and depth	Depth Range	Mean temperature difference (°C) Loggers minus GBR1	Standard deviation (°C)	5th-95th quantiles mean temperature difference
Mooring	47	539,108	10 - 190	0.32	0.52	-0.34 - 1.21
Reef	236	676,671	1 - 10	-0.32	0.35	-0.91 - 0.25

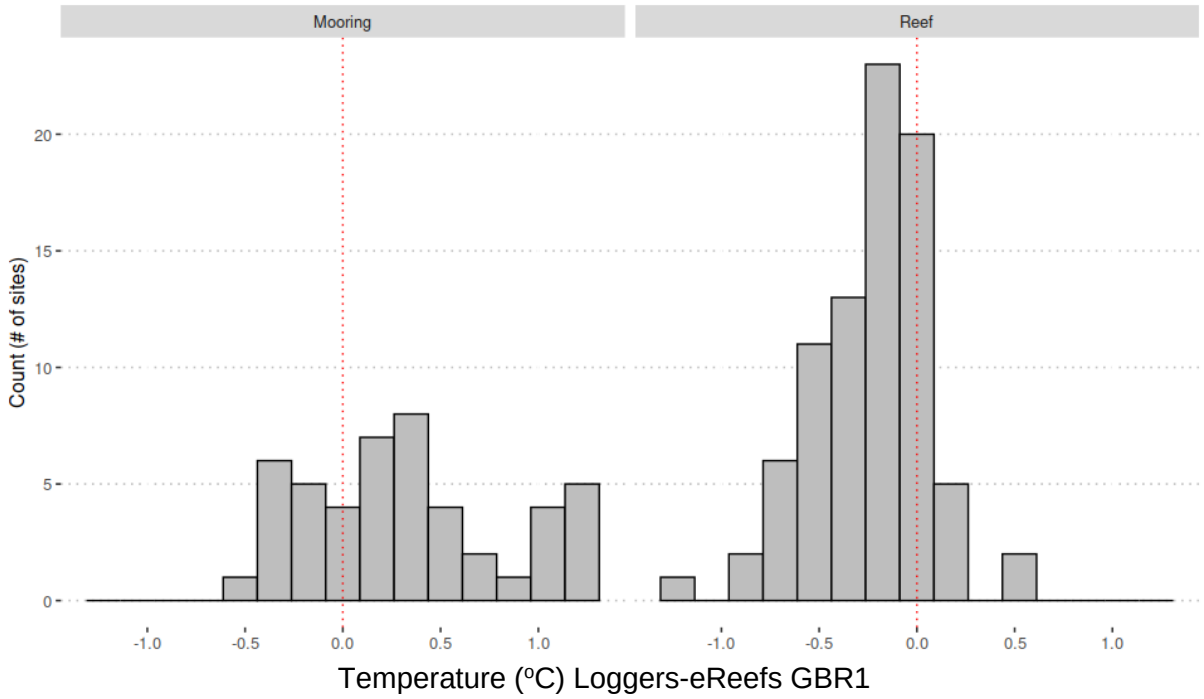

Figure 7: Histogram of the difference between GBR1 temperature time series and temperature loggers at mooring sites (left) and reef sites (right). The vertical dotted line represents the perfect match (difference = 0).

The Willmott's agreement index performed in general very well at reef sites (Figure 8), except at deeper areas (Figure 9). This general metric measures the "goodness of fit" of the model with the coincident observed data and as such, local variations with small spatial and temporal differences between the observations and the model will not be captured by the index, resulting in a lower score.

Herzfeld et al., (2016) noted difficulties in comparing GBR1 output with observations due to the double penalty issue, e.g., Section 5.2.2 Herzfeld et al., (2016) states: 'In areas with large spatial gradients in GBR1, i.e., areas of sub-mesoscale activity, comparison to observation therefore becomes a problem'.

Traditional skill metrics (RMSE, CC, bias etc.) no longer become indicative of true model skill, as resolution increases and small-scale features become more prevalent in the solutions, since small offsets in position of a feature are penalized severely with these metrics as large bias or displacements of a feature. This problem has long been acknowledged in the meteorology community, and neighbourhood techniques have been developed to address the issue. These techniques attempt to overcome the problem by rewarding predictions where the shape and magnitude of a feature are correctly simulated, but it is slightly offset in time or space (Ebert, 2008).

It is likely that comparison of moored instruments with the model is confounded by large, small-scale gradients from sub-mesoscale structure of phenomena such as internal tides and small-scale eddies that cannot be modelled precisely at the same location and time, and that the model bathymetry is gridded to 1km, meaning reef slopes are not well resolved spatially (Herzfeld et al., 2016). We acknowledge that neighbourhood techniques have a role in generating meaningful metrics. This is particularly true of measurement sites located on reef slopes, where mismatches in bathymetry and bathymetric gradient also likely contribute to differences in model-observation comparisons. However, these neighbourhood approaches were not pursued in this study.

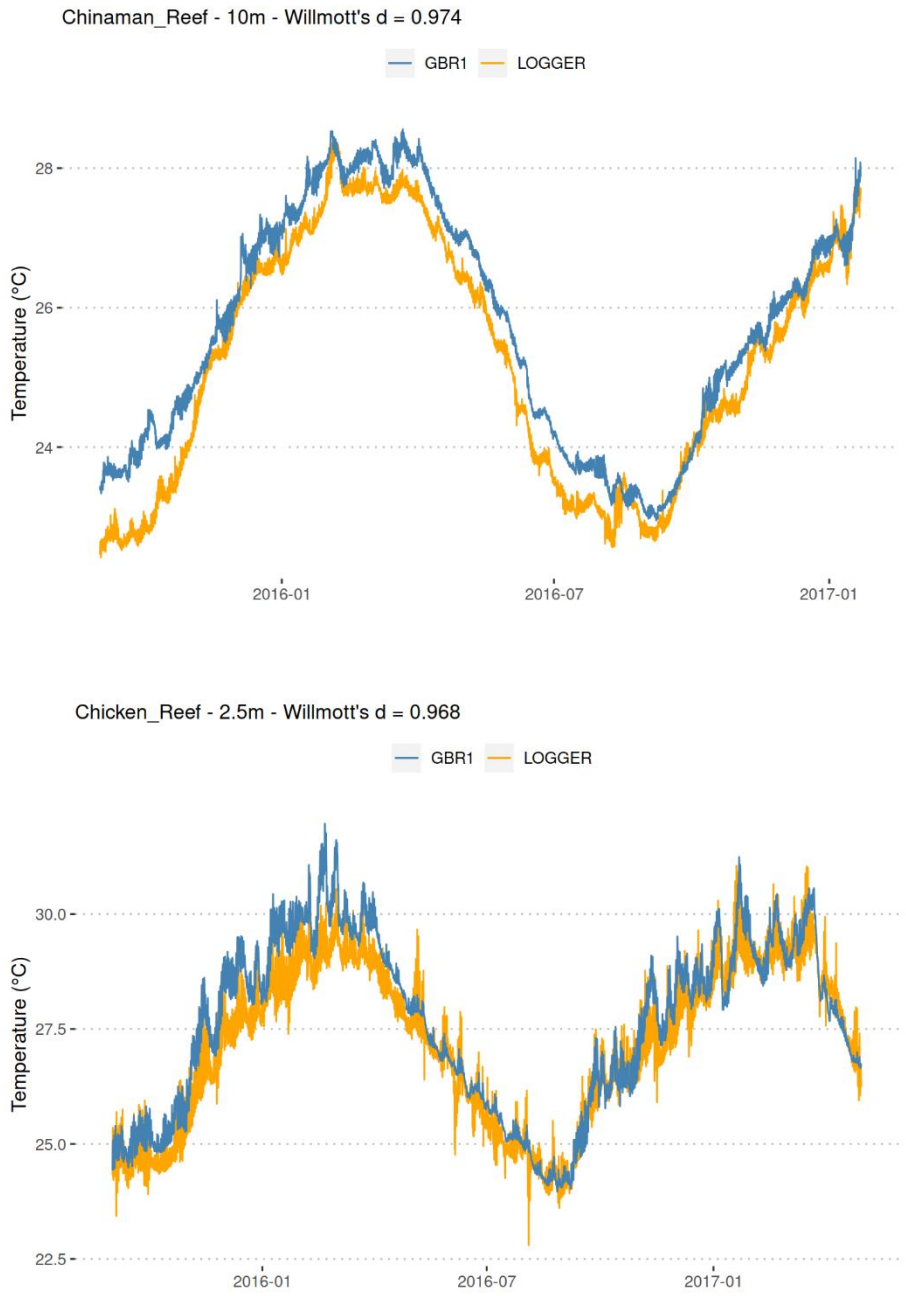

Figure 8: Comparison between GBR1 hourly temperature time series at an example reef slope at Chinaman Reef at 10m (top) and at Chicken reef flat (bottom)

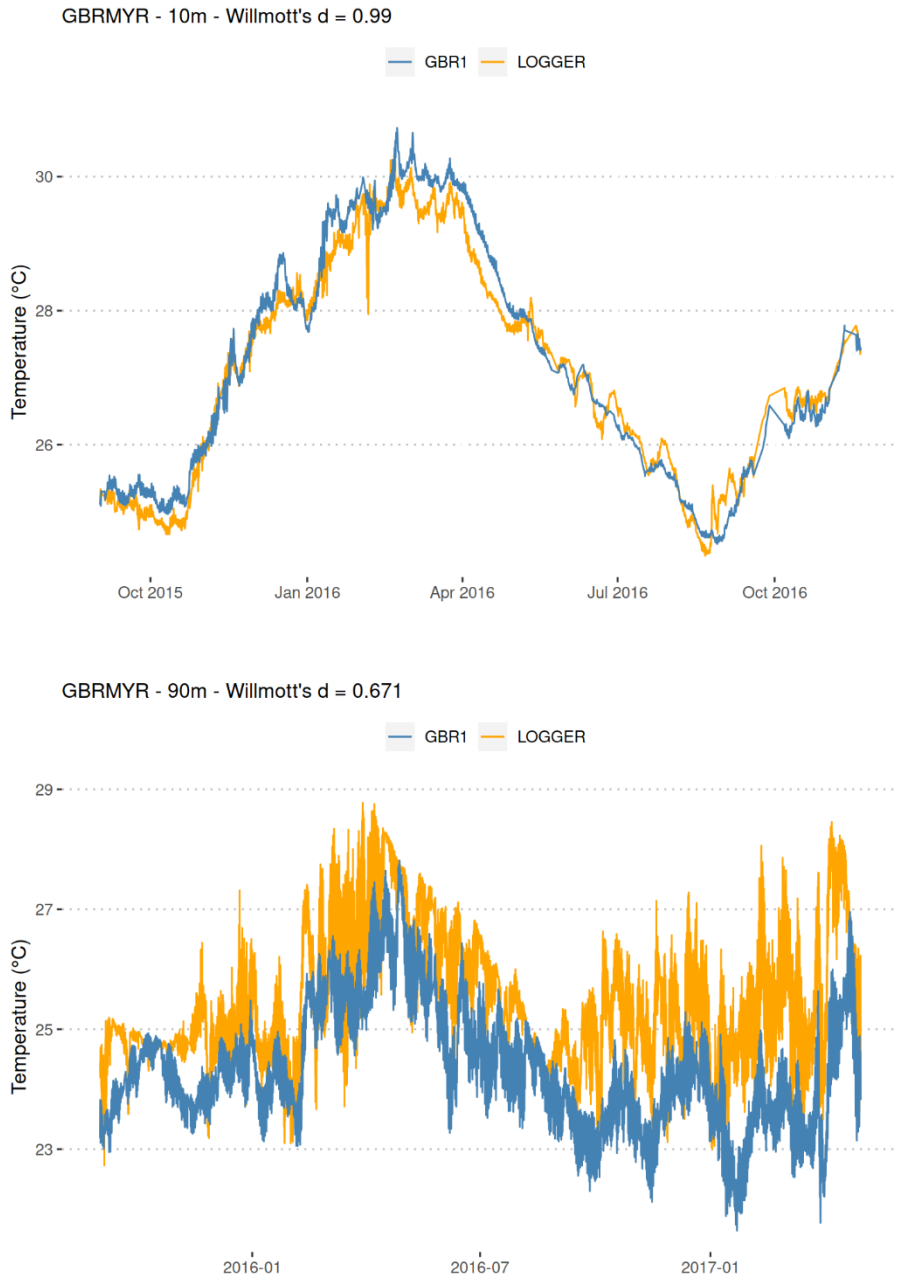

Figure 9: Comparison between GBR1 hourly temperature time series at Myrmidon moored instruments at 10m (top) and 90m (bottom) depth.

3.1.2 Model comparison with satellite data

Comparing the 1km GBR1 predicted values with a 0.054° satellite SST product (GHRSST Level 4 OSTIA Global Foundation Sea Surface Temperature Analysis, https://podaac.jpl.nasa.gov/dataset/OSTIA-UKMO-L4-GLOB-v2.0) shows a good agreement between model and observations (Figure 10). The highest RMSE values are observed near the coast, around the reef locations and where fine scale ocean circulation result in large small-scale temperature gradients not represented in the 0.054° products.

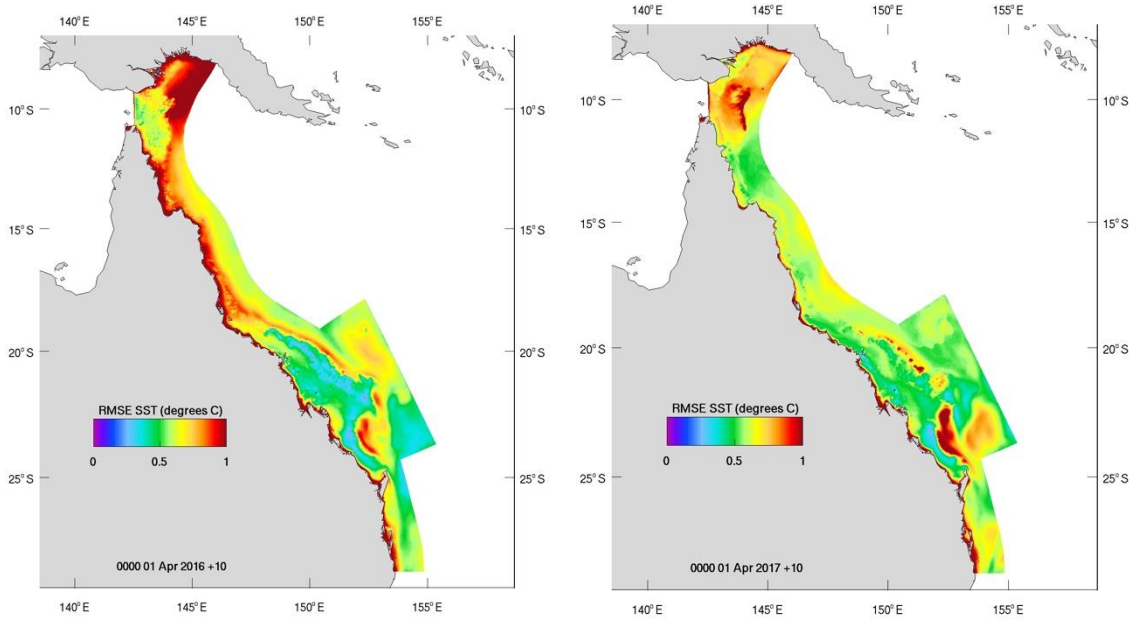

Figure 10: Comparison between GBR1 (~1km resolution) and GHRSST L4 OSTIA (~5km resolution): surface temperature RMSE calculated on GBR1 grid for summer 2016 (left) and summer 2017(right).

3.2 SSTAARS-GBR1 3D climatology

In this section, we analyse the SSTAARS-GBR1 3D climatology and identify potential limitations in the climatological stratification.

3.2.1 Comparison between SSTAARS and GBR1 climatology

As mentioned above, the GBR1 archive is relatively short (December 2014 to present) and not suitable to generate a reliable climatology, since it will be biased by the warmer than usual events in recent years. It is for this reason that we generate a 3D climatology by projecting the SST-derived climatologies throughout the water column using a mean relative stratification profile developed from the GBR1 model (Section 2.2.3). In this section we highlight the shortcomings of a GBR1 climatology that justified the approach of blending SSTAARS with model results.

In Figure 11, we compare the 2015-2019 average GBR1 SST climatology with that from the 1992-2019 SSTAARS climatology on the GBR1 grid for the month of February. The discrepancies between the two February products can have three origins: 1. comparing a 25-year climatology where interannual variability is smoothed out with a more recent 5 years

climatology largely biased towards three marine heatwaves years, 2. misrepresentation of dynamical processes by the model, 3. lower numbers of observations in SSTAARS for the northern GBR during the monsoon season due to the influence of cloud cover.

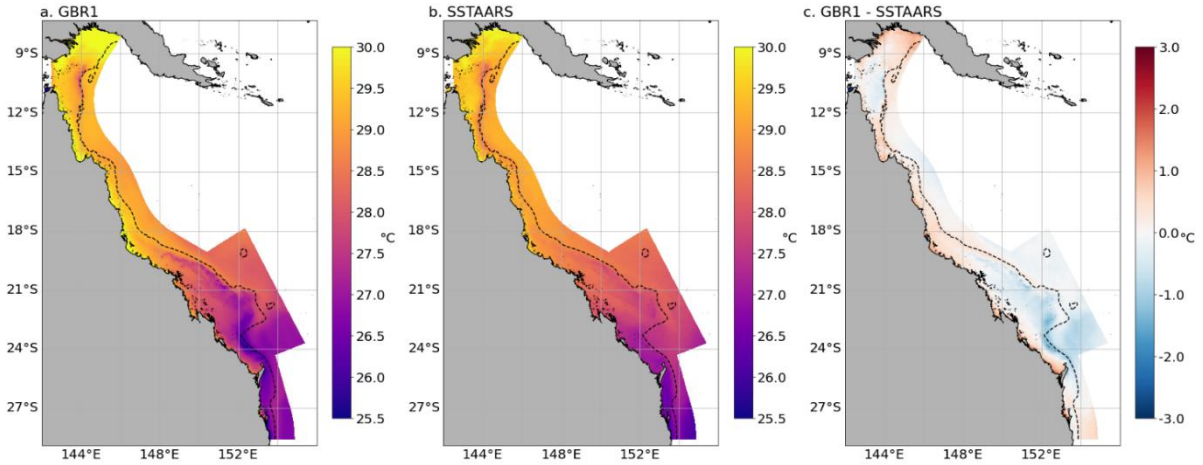

Figure 11: Sea Surface Temperature in GBR - February climatology: 2015-2019 GBR1 climatology (a.), 25-year (1992-2016) SSTAARS climatology interpolated into the GBR1 grid (b.), temperature difference (c.), the black dashed line is the 200m isobath.

Overall, 2015-2019 GBR1 SST climatology is within +/- 0.5°C of the SSTAARS climatology for the month of February, with a few colder hotspots associated with upwelling activities and warm hotspots in shallow areas, along the EAC path and in the Gulf of Papua (Figure 11).

The poleward East Australian Current (EAC) is detected as a warm jet southward from 16°S and shows similar behaviour in the two climatologies. At 19°S, the EAC impinges onto the west-east oriented shelf slope and splits in two: the main jet keeps following the shelf break, while a branch intrudes into the GBR lagoon (Brinkman et al. 2002). Between 19-24°S, the southern GBR lagoon temperature is not only influenced by a warm intrusion in its northern part but also a cold intrusion from the south in the Capricorn Channel at 24°S, creating a strong north-south gradient in the lagoon (Figure 11 left). While the GBR1 climatology represents well the warm intrusion from the north, the cold one from the south is stronger than in SSTAARS. In the southern GBR, the cyclonic Capricorn Eddy is associated with a strong upwelling and cold surface signature at 23-24°S. The 2015-2019 GBR1 climatology shows a 1 to 2°C colder surface signature than SSTAARS. This might be a consequence of the strong upwelling favoured by the exceptional monsoon event in 2019 (Australian BoM Special Climate Statement 69).

In the GBR, the shelf break has a unique SST signature, especially in summer. The interaction of shelf-slope topography with tides, internal waves and strengthened along-shelf currents in summer create regions of strong temperature gradient along the shelf-break and also favour intense mixing and upwelling of sub-thermocline water.

The upwellings result in a cooler water tongue signature along the entire GBR shelf break (Wijffels et al, 2018) (Figure 11 middle), bringing relatively cooler conditions for the outer reefs (Figure 1). The 2015-2019 GBR1 February climatology exhibits cold tongues along the northern outer reefs that are comparable with the 25-year climatology (Figure 11 left). In 2016

and 2017, the GBR also experienced frequent wind generated mixing events and cooling due to near (e.g., Tropical Cyclone Debbie in 2017) and far-field (e.g., Tropical Cyclone Tatiana and Winston in 2016) tropical cyclones.

In the Gulf of Papua, the cold signature is slightly stronger in GBR1 climatology. The shape of this cold intrusion is similar to the observed contribution of the spring/neap tide activity reported in Wijffels et al. (2018), suggesting a consistent tidal mixing response in the GBR1 climatology at this location. However, the cold tongue signature along the central outer reefs is not apparent in the 2015-2019 GBR1 climatology, with GBR1 generally warmer than SSTAARS (Figure 11). This is consistent with the heatwave conditions in 2016 and 2017 (Benthuysen et., 2018), which might bias the GBR1 climatology by suppressing intrusions that would otherwise up well to the surface. The GBR1 climatology shows enhanced temperature near the coast, while SSTAARS shows a more uniform temperature signature in the GBR lagoon.

The differences observed between the SSTAARS and GBR1 climatologies are large enough to warrant the exclusion of the GBR1 products as the basis for a MMM, and an alternative approach is required for generating a 3D climatology.

3.2.2 GBR1 vertical temperature structure

The decrease of temperature with depth is highly influenced by the shelf break, with a stronger vertical gradient along the shelf edge (Figure 12). The Gulf of Papua and the EAC jet are the regions where there is the greatest gradient in temperature with depth, less than 0.5^{o}C at 2.3m deep, 1.2^{o}C at 9m deep and up to 2^{o}C or more at 24m deep (Figure 12). Central GBR is also an area showing stratification offshore and onshore.

As GBR1 displays the shelf currents at their appropriate location, the blending of GBR1 and SSTAARS should create appropriate stratification at these locations. As stated above, the GBR1 profile is a measure of stratification rather than climatology, hence while the GBR1 temperature signature is cooler in the southern GBR lagoon, this should not impact the blended climatology, as there is no stratification associated with the northward cold intrusion at 24°S (Figure 12). In areas of strong upwellings, no stratification is found either. Along the Southern outer reefs area, no vertical gradient of temperature occurs inshore of the EAC (Figure 12). The uniform water column from the surface to 24m deep is due vertical mixing related to the stronger tides and denser reef matrix. The strong upwelling in the Gulf of Papua displays a similar behaviour as well. In the strong upwelling areas, the GBR1 SST biases are not detrimental as it is the absence of stratification that will be passed into SSTAARS.

In the Central GBR, the shelf narrows, and the outer shelf break has a number of reef passages where the reefs are less dense. When the EAC is upwelling favourable, upwelling tends to occur primarily through these reef passages and be confined along the bottom (Benthuysen et al., 2016). Despite the absence of a surface signature, the upwelling mechanisms are present in the model, with the cold signature of the upwelling being apparent from 9m deep in the 2015-2019 GBR1 climatology (Figure 12).

In the Central GBR, the 2015-2019 surface warming signal is stronger than the cooling upwelling signal in the GBR1 climatology. This results in stronger stratification in the Central).

These analyses indicate that the GBR1 mean profile of temperature is consistent with the major dynamics present within the GBR. We can therefore combine the mean temperature distribution with a reliable climatology to project surface conditions to depth and create a 3D climatology. However, the modelled time-averaged stratification in the Central GBR might be too strong. The impact on 3D SSTAARS-GBR1 climatology and 3D MMM needs to be assessed carefully and used with caution.

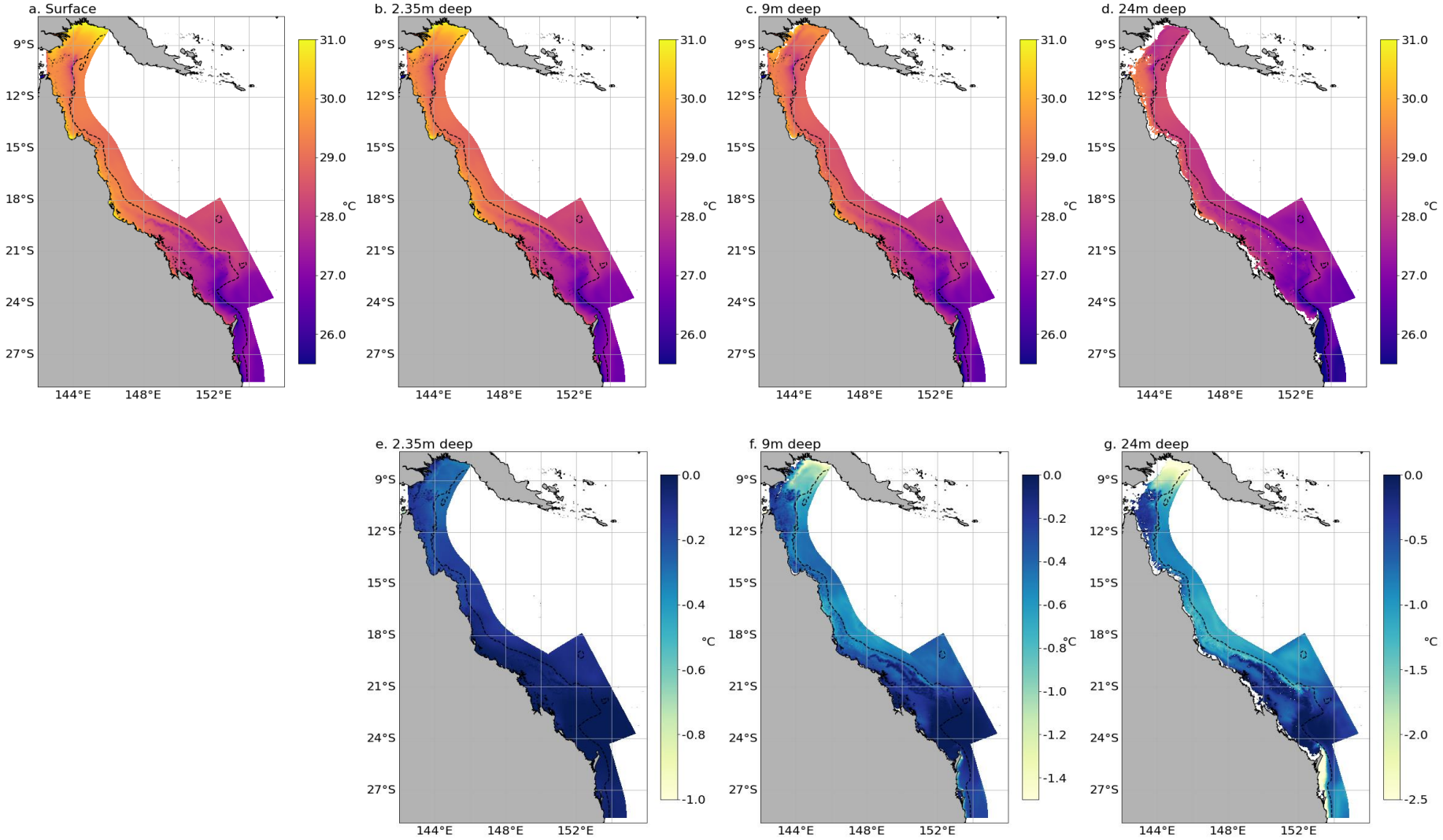

Figure 12: GBR1 vertical temperature structure for the February 2015-2019 climatology SST and temperature at three depths (2.3m 9m and 24m) for the February 2015-2019 climatology (a. to d.), difference between SST and the three depth (e. to g.), the black dashed line is the 200m. isobath.

3.2.3 3D SSTAARS-GBR1 climatology

The GBR1 monthly stratification is used to project SSTAARS at depth. For this product, we keep the climatology centred to year 2005 (Table 1). Results for February and December are shown in Figure 13). The close agreement of oceanographic features between GBR1 and SSTAARS (Figure 11) means that no spurious horizontal temperature gradients are introduced during the projection at depth. Spatial gradients in Figure 13 resemble the spatial gradient in Figure 12. Even for a more stratified month (December), the distinctive north-south and inshore-offshore temperature gradients are maintained. This brings confidence in the use of SSTAARS-GBR1 3D climatology to calculate 3D MMM.

3.3 3D MMM products

We generate two 3D MMM products: one combining the NOAA's Coral reef Watch MMM with GBR1 profiles, and the another combining the SSTAARS-GBR1 climatology with GBR1 profiles. For the MMM products, the surface SSTAARS trend is used to re-centre the product to 1985, while we keep the GBR1 profiles as they are. This means that we assume that the trend is uniform throughout the water column and the stratification did not change over the last few decades.

At the surface, MMM_NOAA is simply the projection of the NOAA's Coral reef Watch MMM onto the GBR1 grid. At the surface, MMM_NOAA and MMM_SSTAARS exhibit similar temperature ranges and a similar large-scale gradient of temperature (Figure 5): in the GBR lagoon, MMM is warmer in the north than in the south. While both products show warmer MMM where the EAC stands and colder MMM where upwellings reach the surface, the difference in the initial resolutions (2km versus 5km) means that the 2km product exhibits more detailed spatial signatures of the features with a stronger horizontal gradient of temperature (Figure 5).

For most depths, MMM_SSTAARS occur in February for a large part of the GBR, except for the Gulf of Papua (Figure 14). For MMM_NOAA, we use the timing of occurrence of the warmest conditions at depth from MMM_SSTAARS, to select the normalized profile use to project the surface MMM_NOAA at depth. As a consequence, the warmest conditions exhibit a similar vertical structure as the averaged February conditions (comparing Figure 12 with Figure 15). Again, thanks to the good agreement between SSTAARS and GBR1, no spurious horizontal temperature gradients are introduced during the projection (Figure 14 left). However, in the Central GBR lagoon, the vertical gradient in 3D MMM between 16-19^{o}S could potentially be an artefact of the GBR1 profiles biased by marine heatwaves in the later years increasing stratification (Figure 15).

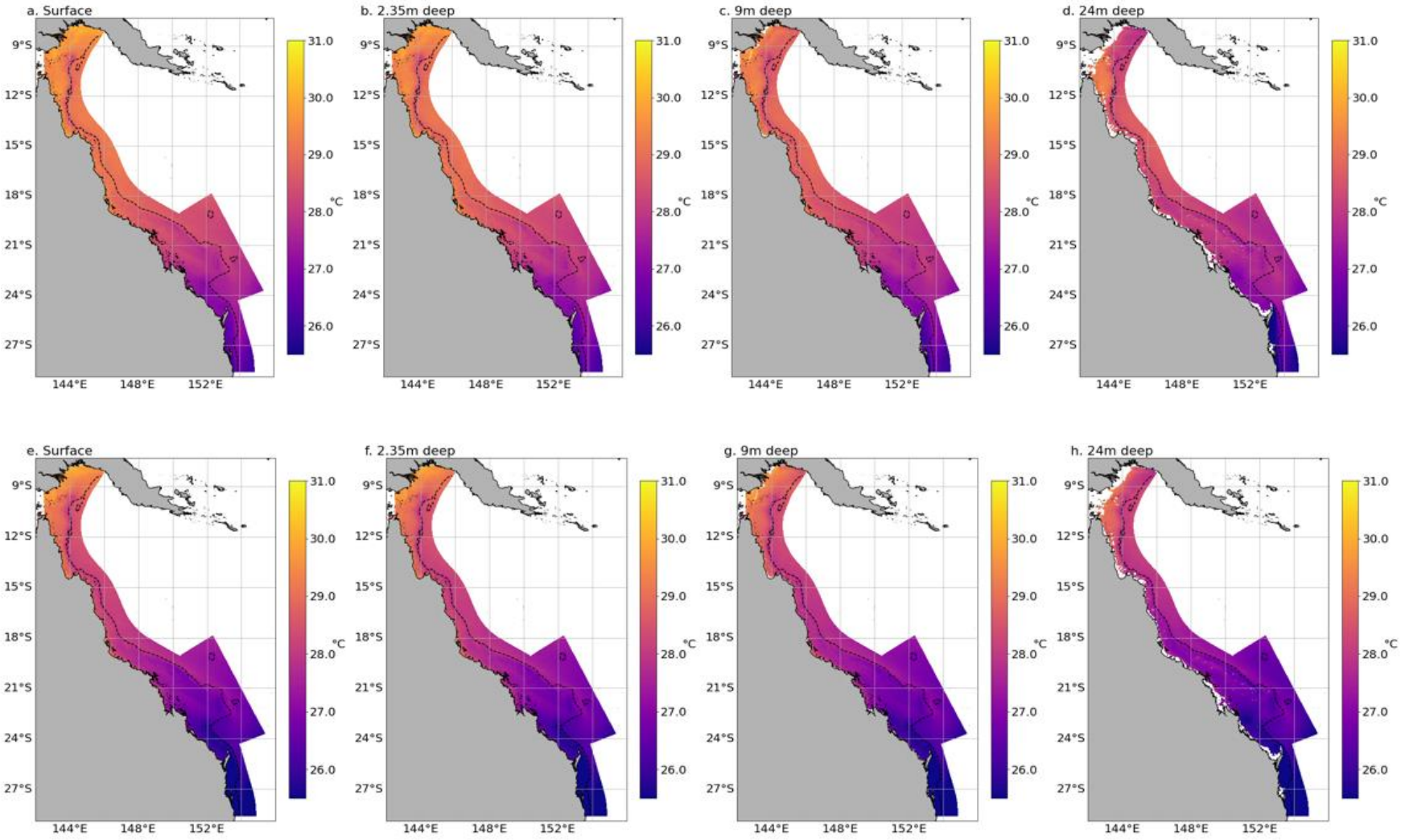

Figure 13: February (top) and December (bottom) 3D SSTAARS-GBR1 climatology (in ºC): SSTAARS at the surface (a. and e.) and its projection at depth using GBR1 profile for three depths (2.3m 9m and 24m). The black dashed line is the 200m isobath.

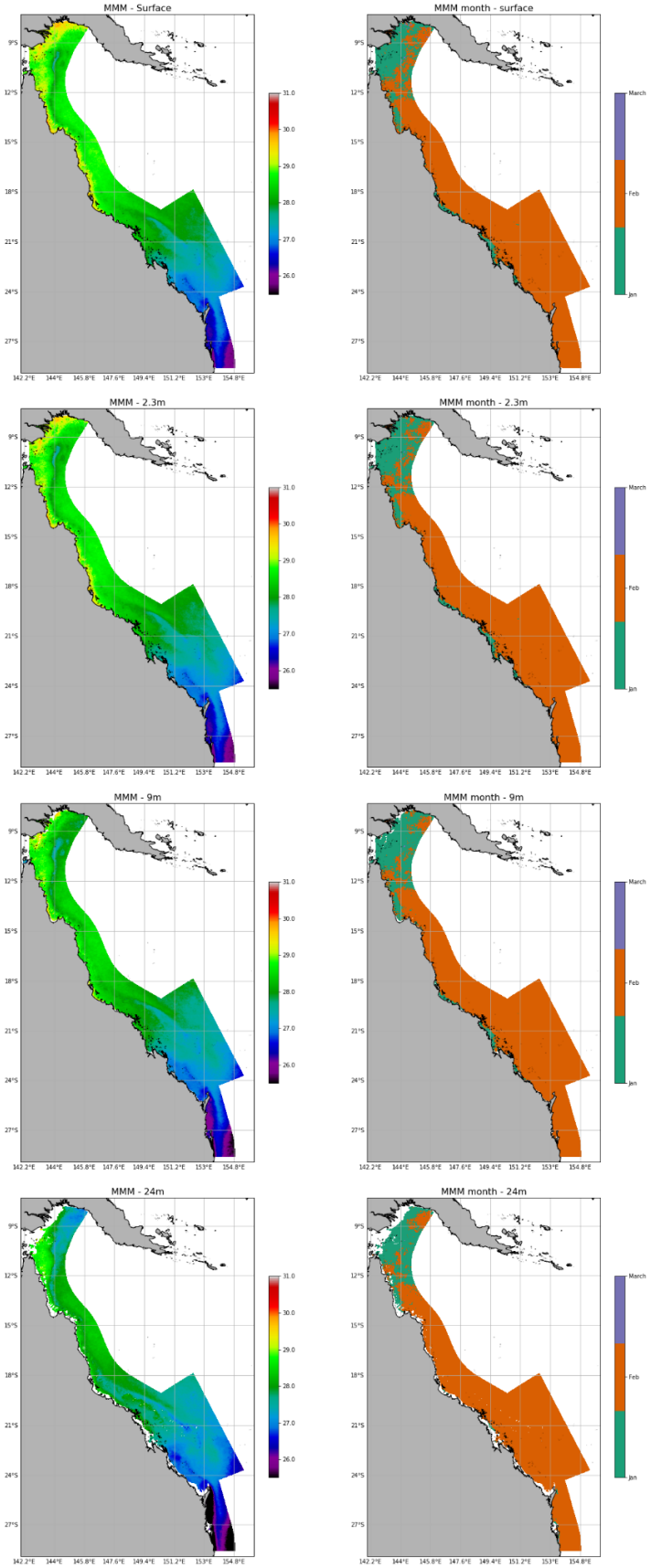

Figure 14: 3D MMM_SSTARS maps: temperature value (left) and month of occurrence (right) for 4 different depths: surface, 2.3m, 9m and 24m (from top to bottom)

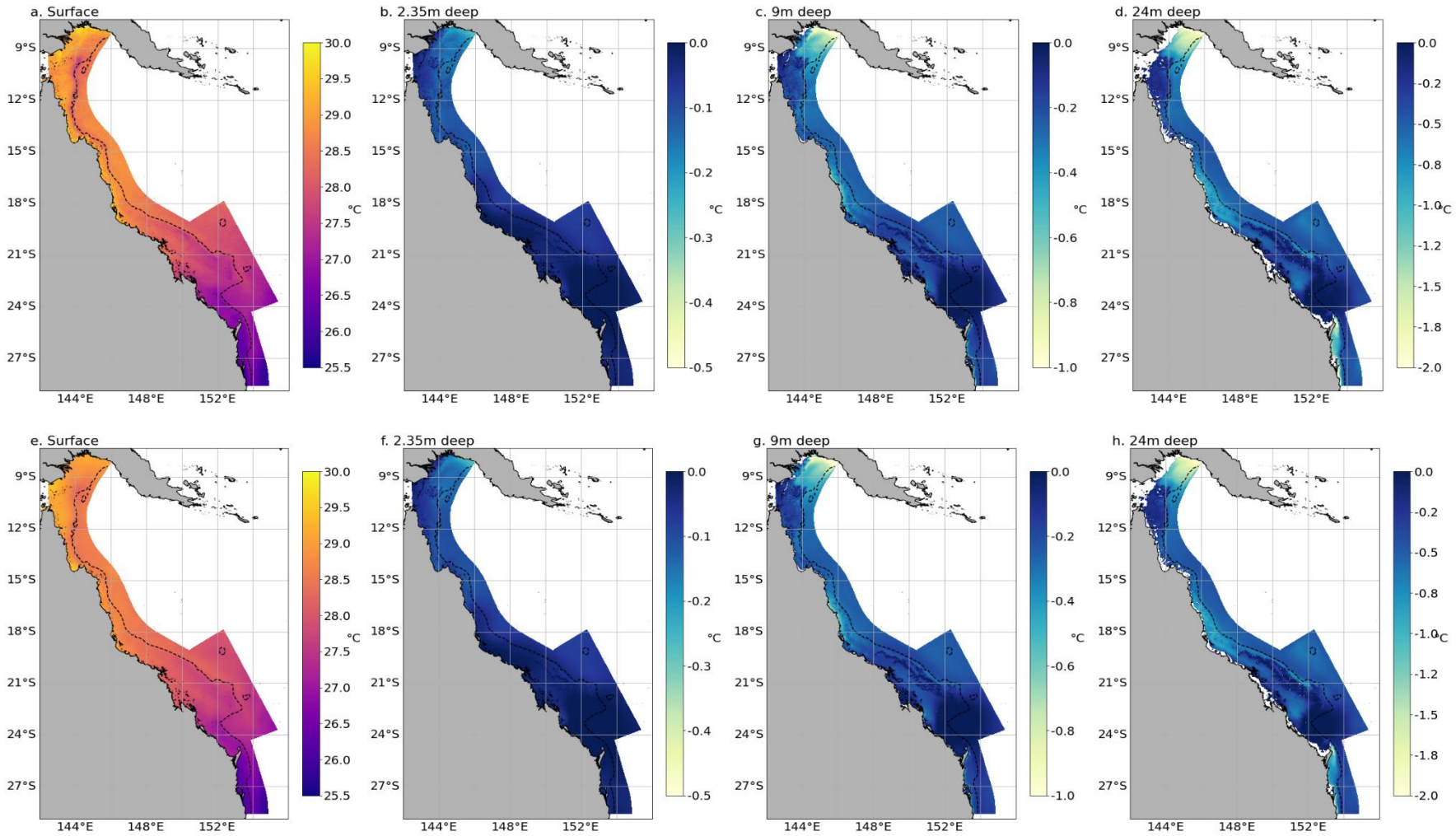

Figure 15: 3D MMM_SSTAARS (top) and 3D MMM_NOAA (bottom) vertical structures: surface MMM (a. and e.) and temperature difference between the surface and three depths: 2.3m (b. and f.), 9m (c. and g.), and 24m (d. and h.). The black dashed line is the 200m isobath.

3.4 3D DHW

3.4.1 Surface DHW maximum

In the GBR, aerial surveys of coral bleaching and the NOAA's Coral Reef Watch DHW (DHW_CRW) show very good agreement in the geographical footprint of the mass bleaching events (Hughes et al., 2017). As a consequence, at the surface, we can compare our two products using GBR1 temperature but with different MMM climatologies, DHW_SSTAARS and DHW_NOAA, with the commonly used surface only DHW_CRW product using satellite SST (see Table 1 for products description). Maximum DHW values over the last five summers (2016 to 2020) are presented in Figure 16 to Figure 20.

The difference between DHW_CRW and DHW_NOAA resides in the daily SST product used to calculate the hotspots: the former uses 5km-daily satellite observation while the latter uses 1km GBR1 SST. The spatial patterns of bleaching risk are well represented by DHW_NOAA, with severe bleaching occurring in Northern GBR in 2016, Central GBR in 2017, and across the three sections of the reef – northern, central and southern - in 2020. This confirms the skilful spatial performance of GBR1 in representing the SST variability and extreme conditions in the GBR. The only mismatches between DHW_CRW and DHW_NOAA are found close to shore along the coast in very shallow areas, where GBR1 is warmer. On one hand, the shallow areas are very sensitive to the parameterisation of the short-wave radiation penetration and GBR1 could be overestimating summer heating; on the other, the 5km satellite product might be degraded at the coast due to land contamination.

The use of the SSTAARS climatology to produce DHW_SSTAARS adds a level of complexity to the spatial resolution of the MMM. As for DHW_NOAA, DHW_SSTAARS correctly represents the spatial patterns of bleaching risk, and the re-centring of SSTAARS results in DHW values similar between the two products, allowing us to use the risk levels defined by NOAA's Coral reef Watch when interpreting DHW_SSTAARS values. However, we note that the ribbon reefs in the far northern GBR shelf break and eastern Torres Strait show severe bleaching using DHW_SSTAARS, especially in 2016 and 2020 (Figure 16 and Figure 20). DHW_NOAA better reflects the DHW_CRW than the DHW_SSTAARS in 2016 (Figure 16). This might be linked to a limitation of SSTAARS in the far north GBR, where the climatology might be too cool.

As GBR1 and SSTAARS introduce finer spatial scales, the transition between low and high DHW values are more abrupt: for examples along the shelf break at 10-11^{o}S and 19-21^{o}S (Figure 16, Figure 17 and Figure 20). The DHWmax distributions at the coral reef locations illustrate this abrupt change in bleaching regime (Figure 21). DHW_NOAA and even more so DHW_SSTAARS tend to have bi-modal distribution, while DHW_CRW distribution is close to gaussian. DHW_NOAA and DHW_SSTAARS have more very low bleaching risk and also more very high bleaching risk, with long tails towards extreme DHW values (Figure 21). These fine spatial scales introduced by GBR1 are consistent with the oceanic circulation which give us confidence that the bi-model distribution is more realistic.

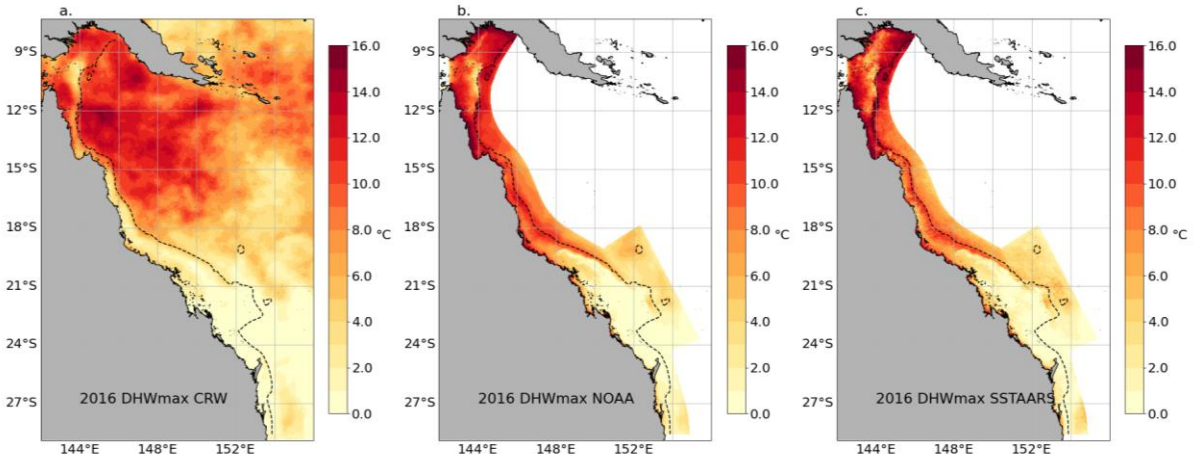

Figure 16: Maximum Surface Heat stress maps for summer 2016: DHW maximum in (°C-week) from NOAA's Coral Reef Watch (a.), Surface DHW maximum using MMM_NOAA (b.) and MMM_SSTAARS (c.). The black dashed line is the 200m isobath.

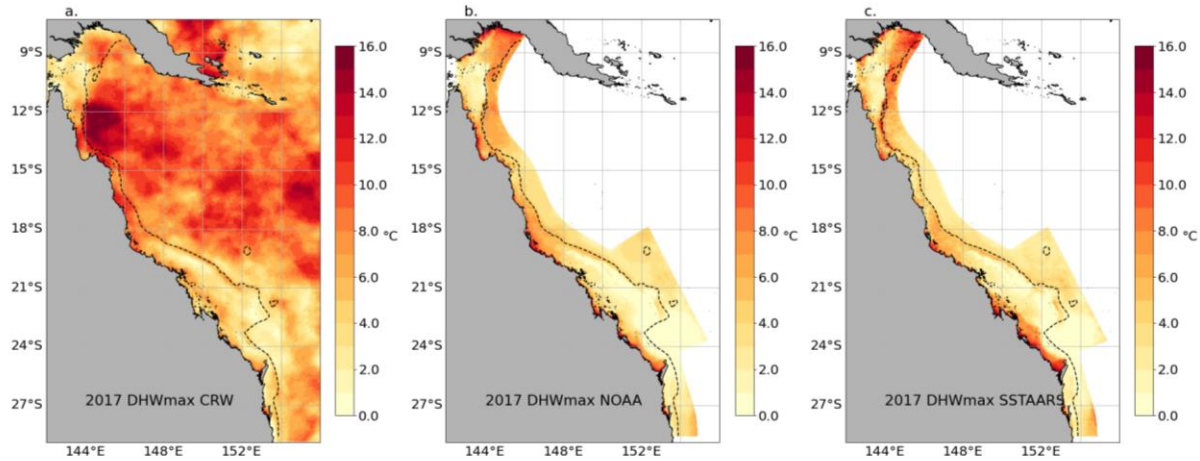

Figure 17: Maximum Surface Heat stress maps for summer 2017: DHW maximum in (°C-week) from NOAA's Coral Reef Watch (a.), Surface DHW maximum using MMM_NOAA (b.) and MMM_SSTAARS (c.). The black dashed line is the 200m isobath.

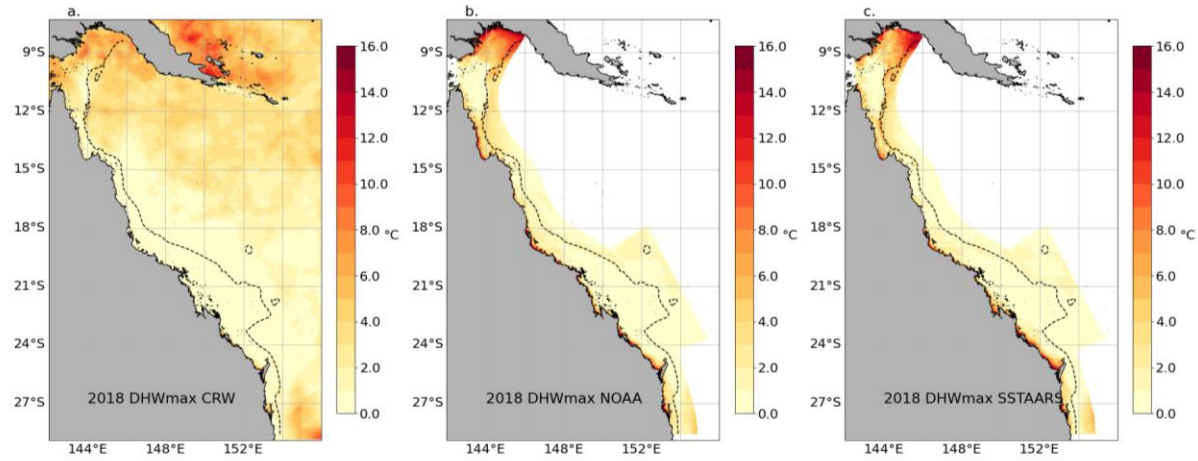

Figure 18: Maximum Surface Heat stress maps for summer 2018: DHW maximum (°C-week) from NOAA's Coral Reef Watch (a.), Surface DHW maximum using MMM_NOAA (b.) and MMM_SSTAARS (c.). The black dashed line is the 200m isobath.

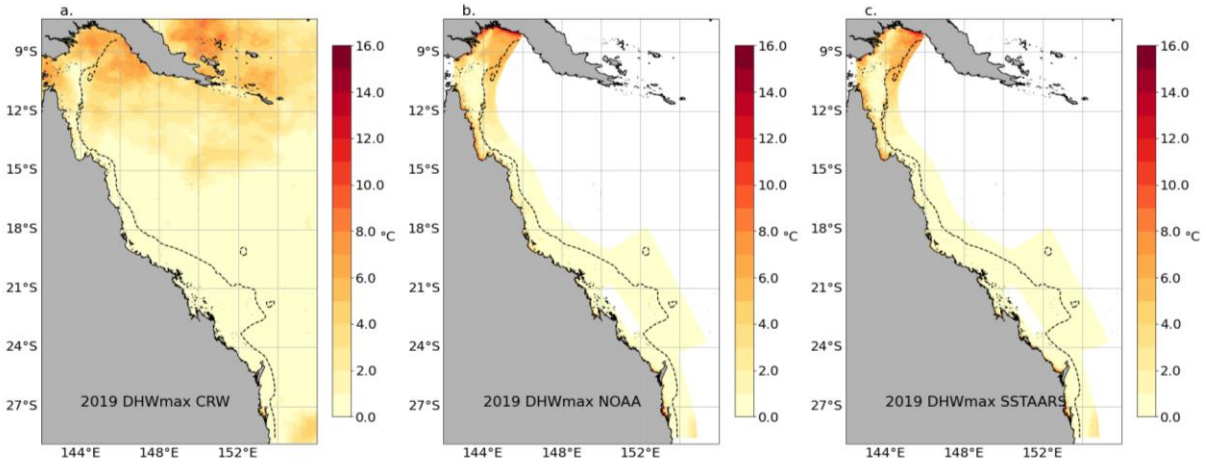

Figure 19: Maximum Surface Heat stress maps for summer 2019: DHW maximum (°C-week) from NOAA's Coral Reef Watch (a.), Surface DHW maximum using MMM_NOAA (b.) and MMM_SSTAARS (c.). The black dashed line is the 200m isobath.

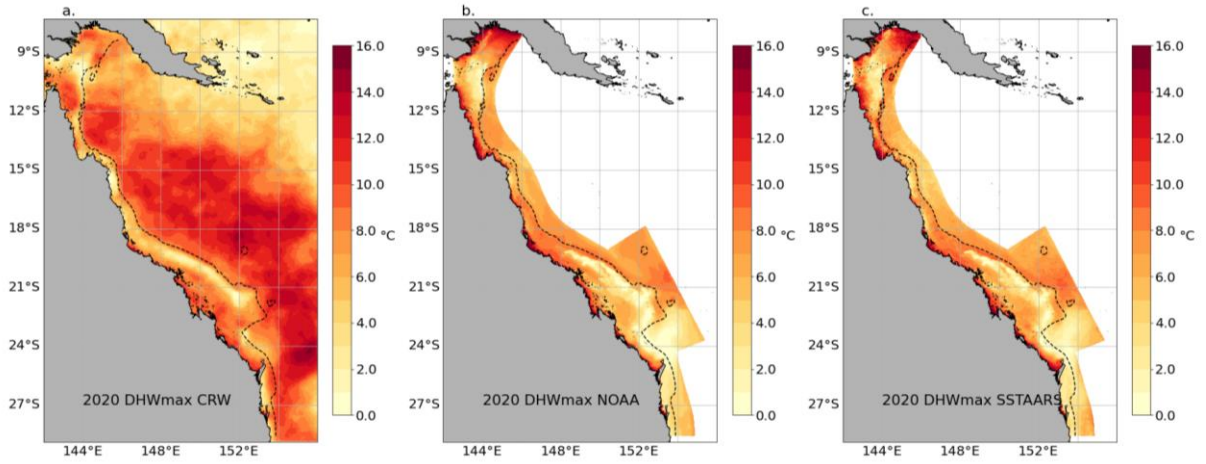

Figure 20: Maximum Surface Heat stress maps for summer 2020: DHW maximum (°C-week) from NOAA's Coral Reef Watch (a.), Surface DHW maximum using MMM_NOAA (b.) and MMM_SSTAARS (c.). The black dashed line is the 200m isobath.

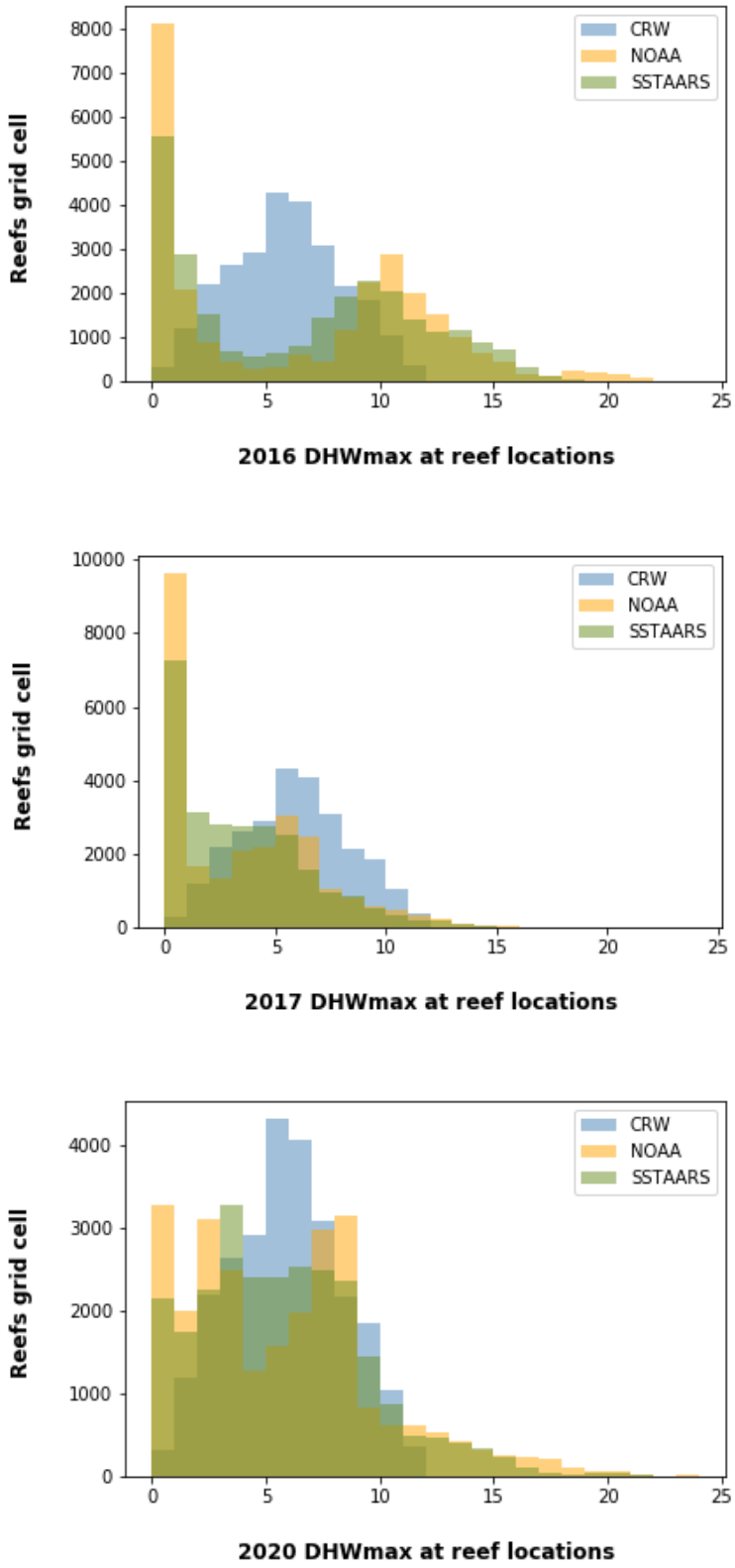

Figure 21: Comparison between surface DHWmax distribution at the coral reefs location: using the NOAA's Coral Reef Watch DHW (CRW) and our two eReefs DHW products (DHW_NOAA and DHW_SSTAARS) in (°C-week) - distributions are shown for the three mass coral bleaching years, 2016 (top), 2017 (middle) and 2020 (bottom).

3.4.2 Refugia versus high-risk areas

Looking at the most recent three mass coral bleaching events (2016, 2017 and 2020), a common trait between bleaching maps emerges: low bleaching risk occurs in areas where upwellings prevail, while high bleaching risk occurs along the shelf break where circulation jets flow (Figure 16 to Figure 20) (see Figure 1 for the surface circulation and upwelling locations). However, while the protected areas occur systematically every year, the high-risk zones can vary from one year to another. Indeed, severity and the annual footprint of bleaching depend on interannual variability in the intensity and coverage of the marine heatwaves, resulting in continental-scale alongshore gradients in bleaching in each particular year.

To better highlight the high-risk zones in the GBR, we combine the footprints of the recent three mass bleaching events, calculating the DHWmax values over the five years for DHW_SSTAARS (Figure 22). While three mass coral bleaching events are not a lot of occurrences, the northern, central and southern GBR have been threatened by severe bleaching once or twice during these events. By combining the footprints of the three mass bleaching events, we artificially impose marine heatwave conditions throughout the GBR. The combined summer maximum DHW results in a situation of severe bleaching risk for the GBR: a footprint of heat accumulation under extreme conditions. This footprint allows us to classify which reefs can be protected from bleaching by regional-scale physical processes in case marine heatwaves occur in their areas.

The resulting map clearly highlights how oceanography modulates the bleaching risk at the scale of the GBR. The shelf-break jets all along the GBR appear as an extended and elongated zone of high bleaching risk (DHWmax > 8°C-week), while upwelling areas appear as refugia (DHWmax < 4°C-week). In Figure 22, 68.5% of the grid cells containing coral reefs (i.e., 17909 cells) experience DHW larger than 4°C-weeks. The remaining 31.5% (8254 cells) are all located in the Southern GBR and Capricorn Channel reefs (Figure 22).

The combined distribution of DHWmax values at the reef locations show two distinct peaks, one centred at 2-3°C-weeks and another centred at 10°C-weeks (Figure 23). These two peaks reflect the sharp changes between high risk and low risk conditions (Figure 22) and are a consequence of the sharp gradient in temperature associated with the oceanographic features (jets and upwelling). The 4°C-weeks limit is defined by NOAA's Coral Reef Watch program as when significant bleaching occurs and can be used to separate the two peaks in the distribution (Figure 23).

Using the heat accumulation footprint, coral reef refugia are only located in the southern part of the GBR, and zooming on the area, they are mainly located in the middle of the outer reef (Figure 24). On the edges of the outer reef, the offshore warm shelf-break jet and inshore warm conditions in the lagoon result in risk of bleaching. In the Capricorn Channel reefs, offshore reefs stay below 4°C-weeks, while more coastal reefs reach high DHW values (Figure 24).

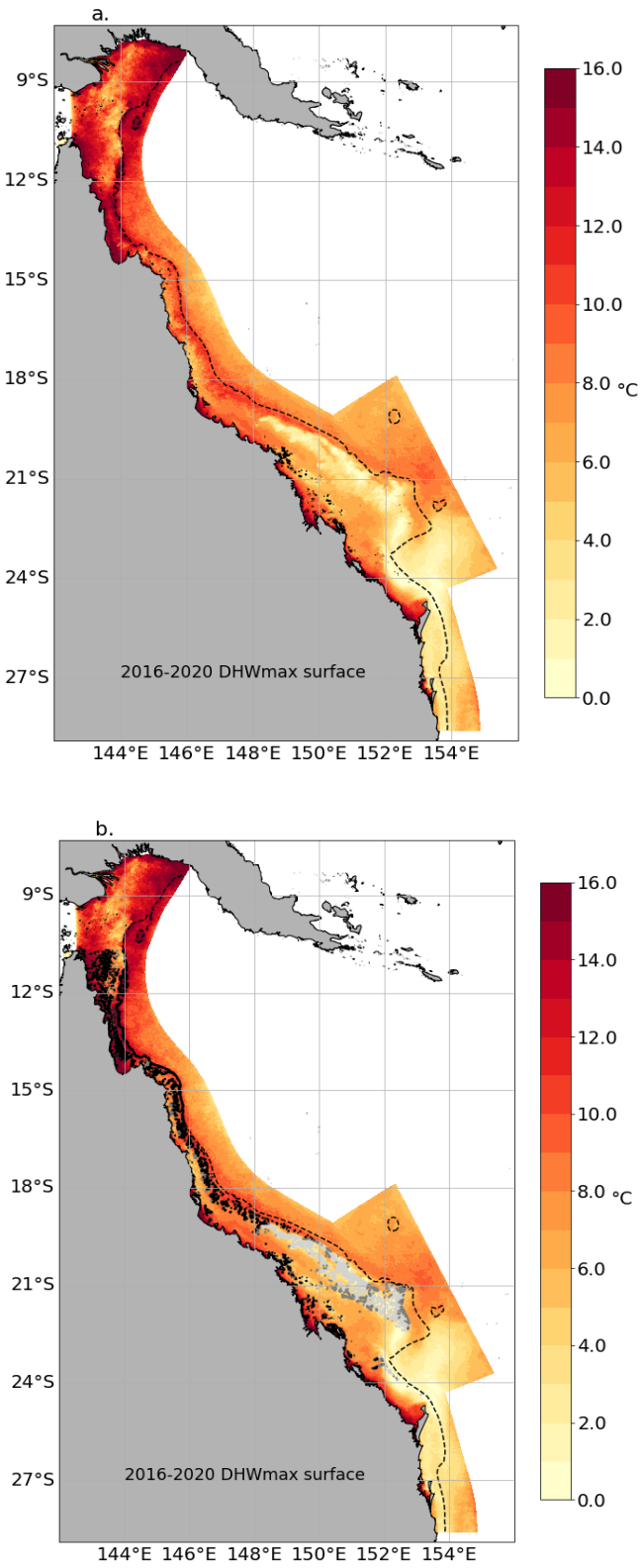

Figure 22: Heat accumulation footprint for extreme conditions: Maximum surface heat accumulation maps for the combined summers (2016 to 2020), using surface DHW_SSTAARS maximum (°C-week). The black dashed line is the 200m isobath (a.), b is the same as a. with the coral reefs cell under severe risk of bleaching (DHW >=8°C-weeks) highlighted in black, under risk of bleaching (4°C-weeks <=DHW <8°C-weeks) in grey and the refugia in light grey (DHW <4°C-weeks).

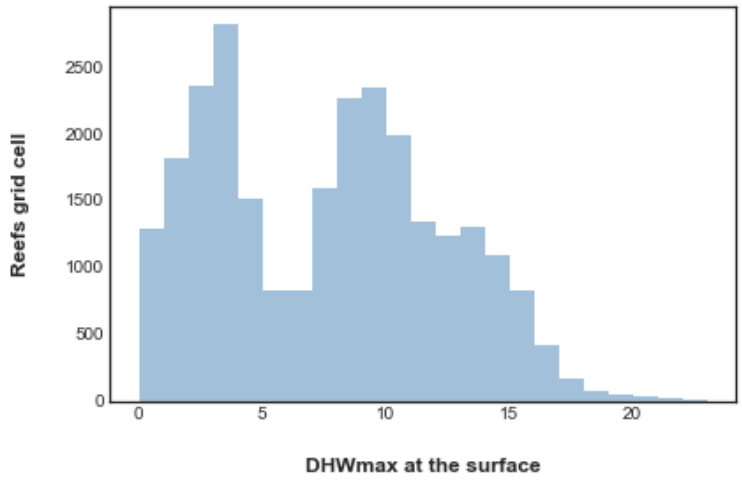

Figure 23: Combined summers DHWmax distribution at the coral reef locations

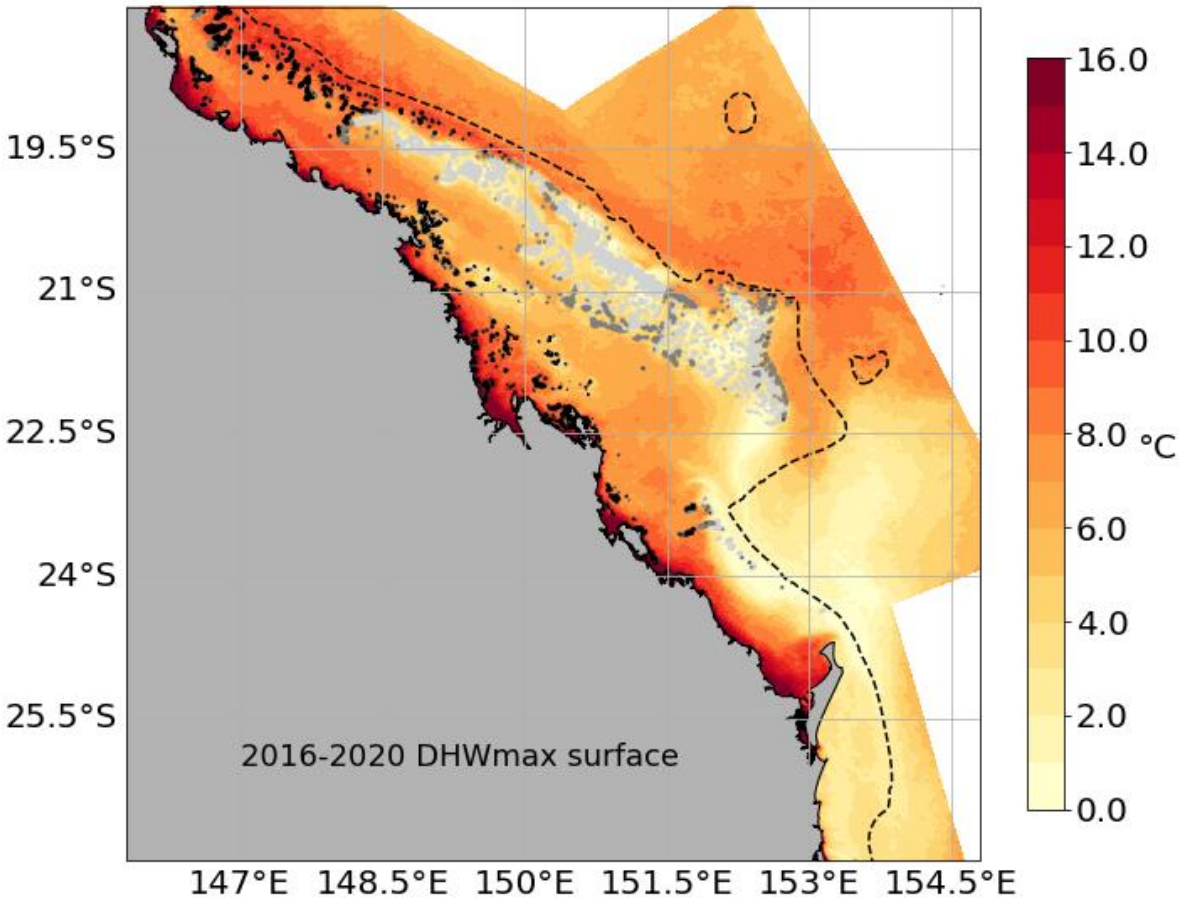

Figure 24: Refugia locations in Southern GBR: as for Figure 22 with the coral reefs cell under severe risk of bleaching (DHW >=8°C-weeks) highlighted in black, under risk of bleaching (4°C-weeks <=DHW <8°C-weeks) in grey and the refugia in light grey (DHW <4°C-weeks). The black dashed line is the 200m isobath.

3.4.3 Comparison of refugia with aerial surveys in 2016 and 2017

While areas of high bleaching risk vary from one year to another, refugia are defined as areas where no bleaching risk is experienced over the years. We use coral bleaching estimations from aerials surveys (Hughes et al., 2017) to assess whether our identified refugia ever experienced bleaching conditions in 2016 and 2017 (Figure 25). In the Southern GBR, some low bleaching category 0 and 1 are consistent in 2016 and 2017 and show the same spatial extend as the surface DHW_SSTAARS maximum: refugia are located in the middle of the outer reef, with some category 2 bleaching occurring on the inshore (in 2016) and the offshore (in 2017) edges of the outer reef. In the Northern GBR, the upwelling area is not identified as a refugia using DHW_SSTAARS, but the level of bleaching risk stays below 8°C-weeks at some reef locations (Figure 22). No bleaching was observed by aerial survey in 2016 in this upwelling area (category 0 bleaching on Figure 25), but unfortunately, the reefs were not surveyed in 2017. These results give us confidence in the use of DHW_SSTAARS to identify refugia in GBR.

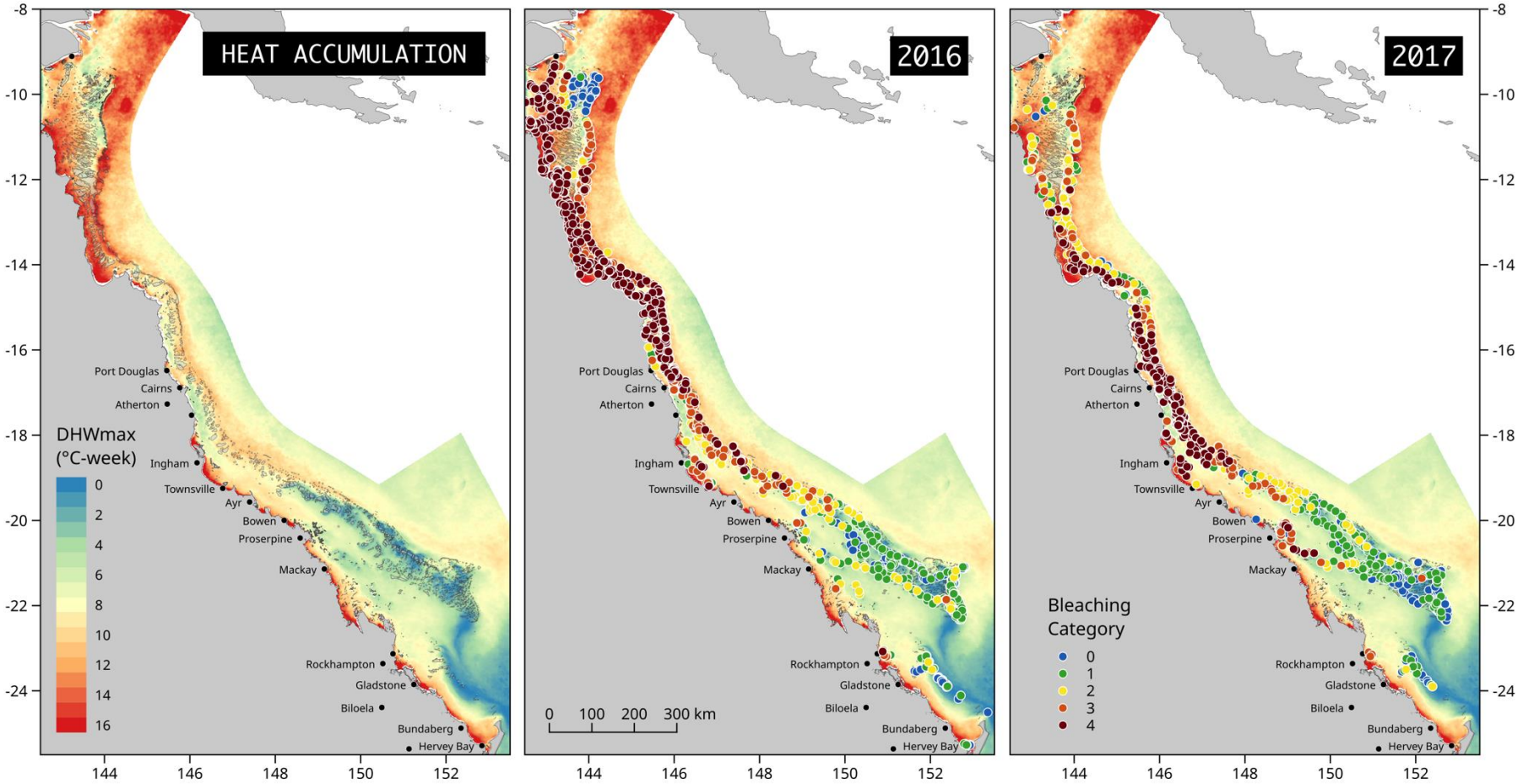

Figure 25: Comparison of 2016-2020 DHWmax with bleaching observations

3.4.4 DHWmax at depth

The use of the eReefs model allows us to explore the bleaching patterns at depths. Here, we present maps of DHW_SSTAARS maximum for five summers and three different modelled depths: surface, 9m and 24m deep (Figure 26 to Figure 30). The upwelling areas exhibit low bleaching risk throughout the water column. At 9m deep, bleaching patterns are similar to the surface with only small reduction in the amplitude of DHW. In 2016, DHWmax at 24m stays very close to the surface values. However, bleaching risk is lower at 24m than at the surface in 2017 and 2020. In particular, the high DHW values associated with the shelf-break jets have reduced at 24m deep. While the shelf-break jets are areas of high bleaching risk at the surface, the stratification within the jets limits the depth to which bleaching conditions are predicted.

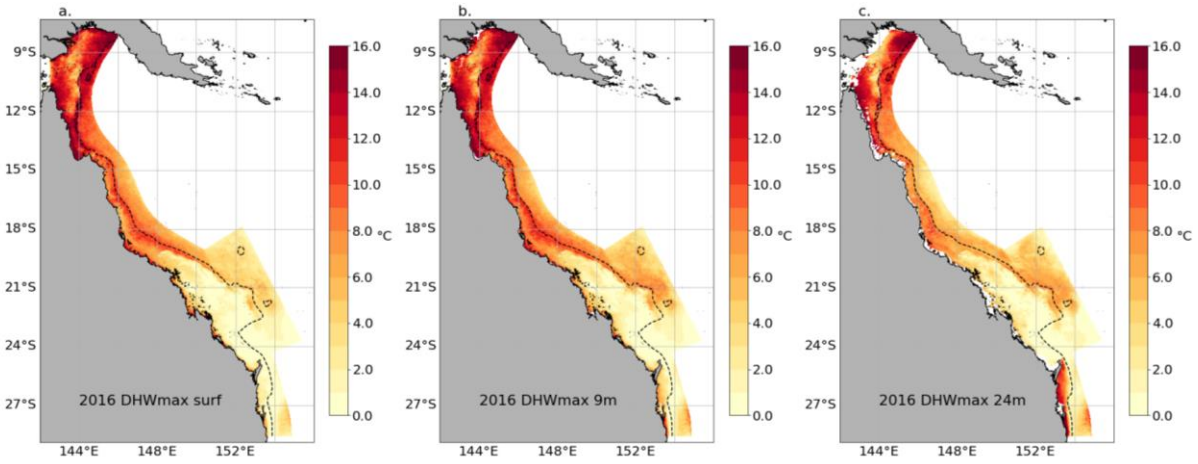

Figure 26: Depth-structure of maximum heat stress maps for summer 2016: DHW maximum in (°C-week) using MMM_SSTAARS for three depths: surface (a.), 9m (b.) and 24m deep (c.). The black dashed line is the 200m isobath.

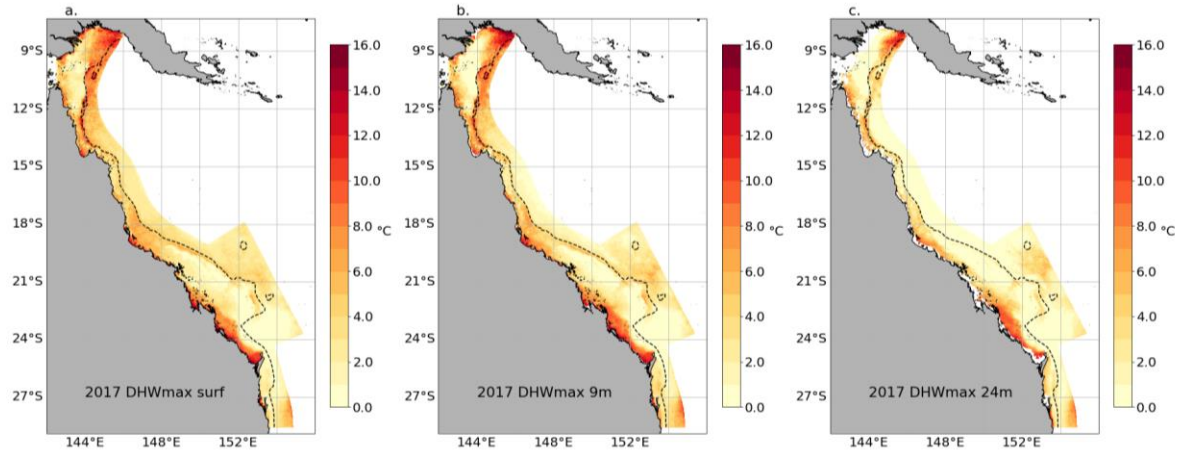

Figure 27: Depth-structure of maximum heat stress maps for summer 2017: DHW maximum in (°C-week) using MMM_SSTAARS for three depths: surface (a.), 9m (b.) and 24m deep (c.). The black dashed line is the 200m isobath.

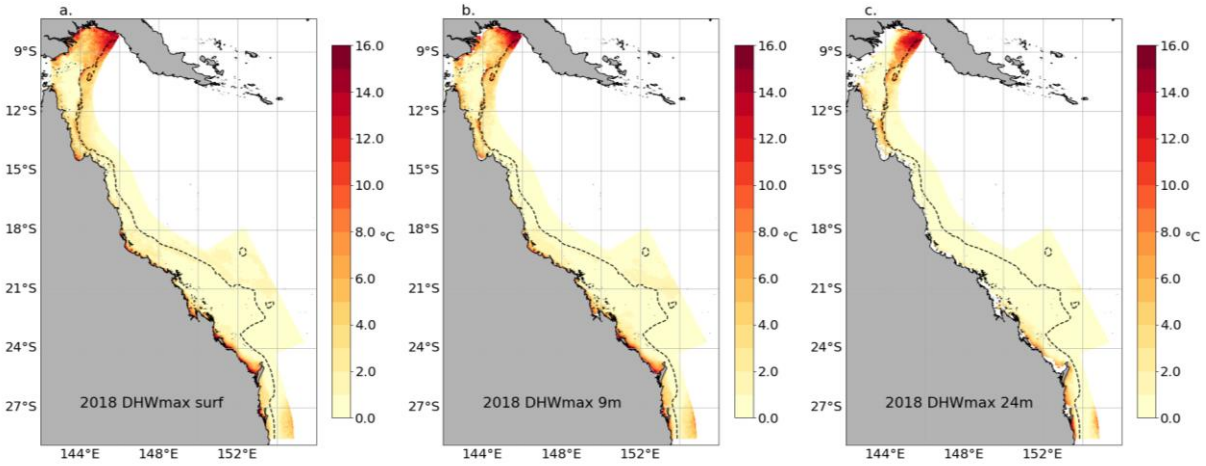

Figure 28: Depth-structure of maximum heat stress maps for summer 2018: DHW maximum in (°C-week) using MMM_SSTAARS for three depths: surface (a.), 9m (b.) and 24m deep (c.). The black dashed line is the 200m isobath.

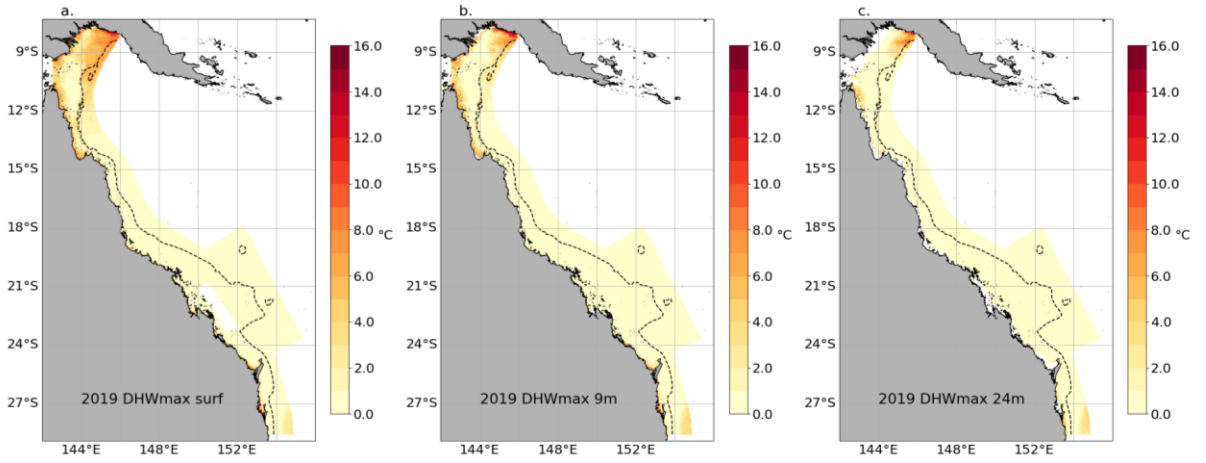

Figure 29: Depth-structure of Maximum Heat stress maps for summer 2019: DHW maximum in (°C-week) using MMM_SSTAARS for three depths: surface (a.), 9m (b.) and 24m deep (c.). The black dashed line is the 200m isobath.

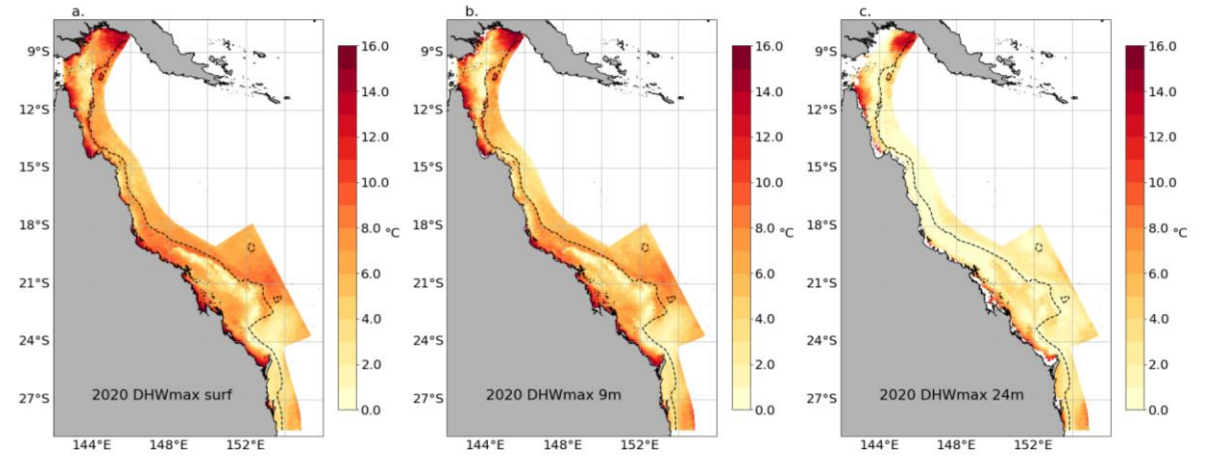

Figure 30: Depth-structure of maximum heat stress maps for summer 2020: DHW maximum in (°C-week) using MMM_SSTAARS for three depths: surface (a.), 9m (b.) and 24m deep (c.). The black dashed line is the 200m isobath.

4.0 DISCUSSION AND CONCLUSION

Limitations of heat accumulation metrics at fine spatial scale

The availability of near real-time remotely sensed SST makes it easy to develop heat accumulation metrics and derived products for the global ocean. However, the accuracy and bias of these estimates have always been a concern. A recent validation exercise showed mean differences of below 0.42°C when comparing different satellite products with Argo floats (Fiedler et al., 2019). The validation process of the satellite-derived SST estimates is done using global drifters, Argo floats, ship of opportunity and moored instruments that are usually at very low density or non-existent in shallow water and near the coast; so, a higher variability and bias could be expected in those areas. This is evident when comparing the GBR1 predicted values with GHRSST OSTIA where the highest RMSE values are observed near the coast, around the reef locations and where fine scale ocean circulation results in large small-scale temperature gradients (Figure 10).

Also, most of the satellite products use night estimates, to access foundation temperature and limit light contamination. As the full diurnal cycle is not accounted for, satellite products might underestimate heat stress, especially for the shallow reef communities. Nowadays this limitation is being gradually removed by the geostationary satellites, like Himawari 8/9, that could produce 10-minute SST estimates, but more validation work is needed at this high temporal resolution. Finally, a spatial resolution of 0.05 degrees for most of the products imposes a limitation on the usability of satellite-derived products in areas like the small and topographically complex reefs of the GBR.

The validation of the GBR1 temperature predictions with *in-situ* loggers has shown at least the same ‘goodness of fit’ that the satellite derived SST has, with the advantage of having a higher (1km) spatial resolution. The comparison with records below 10 metres depth produced higher uncertainties, but this is the result of signals registered by the instruments that are from processes that are not necessarily well represented by the GBR1 model such as internal waves. This is particularly true at sites located on reef slopes, where mismatches in bathymetry and bathymetric gradient also likely contribute to differences in model-observation comparisons. As the main reef communities are in shallow waters (above 15 metres), the GBR1 predictions seem to be very well suited to measure the heat accumulation stress over the GBR at spatial scales of 1km or more.

A new 3D bleaching product for GBR

The objective of this project was to develop and deliver a depth-resolving bleaching product for the GBR, taking advantage of two Australian and GBR-specific products: eReefs 1km hydrodynamical model (GBR1), and the 2km Sea Surface Temperature Atlas of the Australian Regional Seas (SSTAARS).

Two ingredients are necessary to calculate the heat-accumulative bleaching metrics DHW: climatology and daily temperature time series. We combined SSTAARS with 5-year monthly temperature profiles from GBR1 to create the climatology and the GBR1 temperature archive for the time-series. This method has a few advantages:

1. First, this allows us to have a 3D view of the coral bleaching risk, while traditional satellite-based products can only report on the surface bleaching risk.
2. Secondly, GBR1 and SSTAARS improve the resolution of the bleaching product from 5km to 1-2km, allowing us to better resolve the small-scale temperature gradients associated with the circulation. It should be noted that sub-mesoscale phenomena only become apparent at scales of around 1 km or less.
3. Tidal-induced mixing and cooling is represented in the model.

These three characteristics are discussed further in the next sections and compared with previous studies.

A few limitations are:

1. Circulation features create the vertical and horizontal temperature gradients in the GBR. As the GBR1 archive is only 5-years long, a mismatch could exist between the circulation features in the 25-year climatology SSTAARS and GBR1. In the GBR, the strong temperature gradients are created by the shelf-break jets that propagate warm water coming from the Southern Equatorial Current, by wind-driven upwelling as well as by thermocline uplift due to impinging jets, eddies or tidal mixing. As these mechanisms are locked by the geometry of the shelf break, no major horizontal mismatch was found for the location of the oceanographic features between GBR1 and SSTAARS. However, stratification in Central GBR could have been over-estimated by GBR1. Between Cairns and Townsville, the upwelled water does not always reach the surface (Benthuysen et al., 2016). As three of the 5-year simulation of GBR1 occur during marine heatwaves years, no surface signature of the upwelling is apparent in the GBR1climatology (Figure 3). An enhanced stratification in Central GBR could translate to a reduction in the DHW values at depth. As relatively high DHW values are found at depth in the central GBR (Figure 26 to Figure 30), we conclude that the size of the 5-year GBR1 archive is not detrimental.
2. To obtain DHW values comparable with NOAA's Coral reef Watch, we had to re-centre SSTAARS 20 years back in time, using the trend provided in SSTAARS. It is important to note that this trend is interannual and not seasonal. Heron et al. (2017) used a seasonal trend to re-centre the NOAA climatology. Moreover, we assumed no decadal changes in stratification.
3. Since SSTAARS might be impacted by cloud cover, the summer climatology as well as the trend might be impacted by the amount of available observations in summer, in particular in the Northern GBR.
4. Finally, it is well-known that in an area of low seasonality, the timing of the seasonal peak may vary from year to year. As a consequence, the long-term mean of the maximum monthly SST from each year (MMMmax) is a better measure of the typical warmest temperature than the monthly maximum mean (MMM), especially in the northern part of the GBR. The direct utilisation of the SSTAARS climatology did not allow us to use MMMmax as thermal threshold. This could have led to an underestimation of MMM and an overestimation of DHW values in the northern part of the GBR.

Overall, this study shows that using MMM_SSTAARS centred in 1985 and GBR1 SST, provides a viable DHW product, with the highest spatial resolution possible. For this DHW product we used a midnight daily snapshot of SST for the calculation of hotspots.

Another advantage of using a model is, that the hotspots can be calculated at every model time-step, allowing us to integrate the heat accumulation at a much higher temporal scale. The snapshot and integrated DHW products are now routinely provided as outputs from the GBR1 NRT model and will be accessible through the eReefs portal (https://ereefs.org.au/ereefs) as well through the e-atlas (https://ereefs.aims.gov.au/ereefs-aims/gbr1/dhw_heatstress). It is important to note that, the daytime hotspots are likely to be larger than the night-time ones, resulting in much larger DHW values for the integrated DHW products. As a consequence, the DHW limits defined by the NOAA Coral reef Watch won't apply to these integrated DHW metrics. These new products need to be calibrated against observations to understand the risk category limits but should be more representative of the actual thermal stress corals experience due to diurnal variability.

Identifying refugia

The challenge in determining which parts of the GBR could potentially be a refugia is that geographic bleaching footprints are influenced by different phenomena that vary from year to year. Warmer than usual temperatures result from a combination of background climate warming, climate modes of variability like the El Niño Southern Oscillation (ENSO), as well as local processes. For the past decades, multiple studies focussed on understanding the processes behind bleaching risk in the GBR. For example, ENSO is associated with changes in air-sea fluxes with weakened monsoon and reduced cloud cover (Lough 1999; Benthuysen et al., 2018) and also impacts circulation, stratification and heat transport (Kessler and Cravatte, 2003; Benthuysen et al., 2018). At local scales, processes impacting SST include not only weather conditions (tropical cyclone, anomalous cloud cover and wind) but also changes in heat transport by currents (Carrigan and Puotinen, 2014; Leahy et al., 2013; Feng et al., 2003). These complex interactions make prediction of areas of high bleaching risk challenging, and as a consequence identification of refugia is still under debate in the GBR.

Internal tides and their associated vertical mixing can counteract the effect of warming and has been shown to slow down the trajectory towards recurrent bleaching (Storlazzi et al., 2020). Depth has also been proposed as potential refugia (Bridge et al., 2014; Baird et al., 2018). At the scale of a reef, Green et al. (2019) also shows that localised dynamical ocean processes can protect reefs from heat stress and bleaching (at Scott Reef during summer 2016).

A common characteristic of the proposed refugia is a weak temperature variability and very little extreme conditions. In this study focussed on the GBR, we show how dynamical ocean processes can modulate and reduce the heat stress at the scale of the GBR. In particular, we show that upwelling areas in the GBR have been consistently acting as a mitigating factor to bleaching during the past mass coral bleaching events. Upwellings can result from a few processes: wind-induced upwellings, enhanced mixing of sub-thermocline water due to interactions between the shelf-slope topography with tides and internal waves, and thermocline uplift due to along-shelf currents.

While tide-induced mixing tends to reduce heat stress in the far northern GBR and eastern Torres Strait (Figure 22), we found that the only area staying below 4°C-week at the surface is the southern outer reef which is protected by the EAC-induced upwelling. While the current-driven thermocline uplift is the primary mechanism to deliver cool water from depth to the outer slope (Figure 24), the strong regional tides and densely packed reef matrix provide channelling of the flow and mixing, allowing the cooler waters to reach the surface. In the Central GBR, the EAC and tides are not as strong as further south, and the uplifted cold waters do not reach the surface and are therefore called intrusions. While surface areas in the Central GBR experienced high bleaching risk during the past mass bleaching events, the sub-surface intrusions have the capacity to protect areas below 24m.

Interestingly, we find that the circulation patterns are not only dictating where refugia sit but also where zones of high-risk are. The ribbon of high risk along the shelf break in Figure 22 highlights the warming signal carried by the shelf currents. This is consistent with Kessler and Cravatte (2013), and Schiller et al. (2009) that show that besides air-sea fluxes, heat gain by horizontal advection can also be predominant in modulating extreme SST events in the GBR. The strong stratification of the along-slope currents means that below 24m, the high bleaching risk associated with the current vanishes.

The EAC plays a double game: it is a medium for advecting extra heat as well as a trigger for cooling. The association of thermocline uplift and tidal mixing brings cooler waters to the surface and channels them on the continental slope between the outer ribbon reefs, providing a ribbon of persistent tidally modulated cooling. A consequence is that zones of high and low bleaching risk are adjacent to each other and high spatial resolution is needed to contrast these areas. While our DHW products clearly have sharp gradients of temperature and double peaks distribution of DHWmax, the satellite-based Coral Reef Watch product does not. The Coral Reef Watch product is a very useful tool for globally monitoring current and potential future bleaching threats. However, the 5km resolution is not enough to capture fine-scale circulation pattern, resulting in bleaching patterns that are smeared out, limiting the ability to identify refugia. Even at the scale of the Coral Sea, coarser resolution products can show disparate bleaching patterns (see Figure 2 of DeCarlo and Harrison, 2019).

In our study we adjusted the thermal threshold at depth using monthly mean vertical profiles from GBR1. We found two major processes influencing the modulation of bleaching risk at depth: the sub-surface intrusions in Central GBR and the stratification of the along-slope jets in concert with the tides. For both, 24m appears as the limit below which deeper reefs may escape heat stress experienced at the surface (in particular in 2017 and 2020 with the exception of 2016). These results differ from the studies of Smith et al. (2016) and Venegas et al. (2020) that did not find any depth refugia. While Venegas et al. (2020) found stratification at some observation sites (i.e., depth-dependent cooling), the studied sites experienced strong temperature variability at depth. The observed variations throughout the water column resulted in heat stress at depth. In our case, the dynamical processes counteract the warming signal, weaken the temperature variability and inhibit the heat stress at depth.

The vulnerability to climate variability and trend is key to understand refugia. The common trait of the surface and deep thermal refugia identified in our study is the presence of dynamical processes that counteract extreme conditions thanks to mitigating cooling effect.

It is important to note that the refugia would last, as long as the cooling processes are strong enough to counteract warming. As in Frade et al. (2018), we find that in 2016 the warming penetrated deeper, showing the limitation of the deep reefs refugia. As soon as surface warming overrides the cooling from the deep, it is likely that severe heat stress will be experienced at depth. Moreover, the corals in the upwelling areas experience cooler and less variable conditions than the rest of the GBR, which might limit their capacity to adapt to rapid changes.

5.0 RECOMMENDATIONS

5.1 Use of eReefs model for monitoring past, current and potential future bleaching threats

Historically, the 1998, 2002 and 2016 mass coral bleaching in the GBR have been associated with the positive phase of El Nino. However, in recent years, mass coral bleaching events in 2017 and 2020 occurred while ENSO was neutral. As the climate continues to warm, the positive phase of the climate mode is no longer an index of bleaching risk in the GBR. This 2020-2021 season, a moderate La Nina peaked in January and brought cooler conditions to the GBR. SST are predicted to be below averaged in January-March 2021, with gradual easing towards neutral values expected during the first quarter of 2021 (http://www.bom.gov.au/climate/enso/outlook/).

As we move towards a warmer state, the question is no longer whether and why coral reefs bleach, but whether there exists, regions that are insensitive to climate variability and trends, i.e., low variability areas that could act as refugia. Here we show that use of the 1km eReefs model is the best product to identify these refugia. As the refugia are influenced by small-scale oceanographic features, the 1-km resolution of the modelling product is paramount.

Our recommendation is to use the DHW product from eReefs for monitoring past, current and potential future bleaching risks.

5.2 Use of the SSTAARS-GBR1 3D climatology for assessing temperature anomalies from observations.

There are few climatologies available accounting for temperature variations with depth, and their resolutions are not fit-for-purpose in the GBR: CARS climatology has a 0.5° horizontal resolution and the Australia Shelf Seas Atlas a resolution of 0.25°. The SSTAARS-GBR1 3D climatology has the potential to fill this gap for the GBR. It has already been used to assess temperature anomalies from glider measurements in the southern GBR, deployed at the end of the 2020 marine heatwave (IMOS Ocean Currents Newsletter http://oceancurrent.imos.org.au/news.php#Glider_reveals_extreme_heating_to_40m_depth_on_the_Southern_GBR). The use of the SSTAARS-GBR1 3D climatology allows us to follow the evolution of subsurface temperature anomalies.

We note that the SSTAARS-GBR1 climatology would benefit from a longer GBR1 hindcast, in order to bring the modelled period closer to the SSTAARS period. This would improve the product so that it was not as sensitive to more recent events and accelerated warming, in particular in the northern GBR.

5.3 Access and publication of new products for Reef managers and Stakeholders

The DHW products from eReefs GBR1 should be easily accessible by reef managers and stakeholders. Four DHW metrics are now routinely calculated by GBR1 Near-Real Time model and published on the NCI portal (http://dapds00.nci.org.au/thredds/catalogs/fx3/catalog.html): the two snapshot metrics presented in this report, and two integrated metrics.

The two, snapshot metrics are:

- The 3D DHW_NOAA – DHW metric using the NOAA MMM at the surface and 4am snapshot of temperature for the hotspots' calculation.
- The 3D DHW_SSTAARS – DHW metric using SSTAARS MMM at the surface and 4am snapshot of temperature for the hotspots' calculation.

A significant advantage of using a model is that the hotspots can be calculated at every model time-step, allowing us to integrate the heat accumulation at a much higher temporal scale. It is important to note that, the daytime hotspots are likely to be larger than the night-time ones, resulting in much larger DHW values for the integrated DHW products. As a consequence, the DHW limits defined by the NOAA Coral Reef Watch do not apply to these integrated DHW metrics. However, the integrated metrics should be more representative of the actual thermal stress corals experience due to diurnal variability.

The two integrated products are:

- The 3D integrated DHW_NOAA - DHW metric using the NOAA MMM at the surface and hotspots calculated at the model time-step.
- The 3D integrated DHW_SSTAARS - DHW metric using the SSTAARS MMM at the surface and hotspots calculated at the model time-step.

The new products will also be accessible through the e-atlas portal (https://ereefs.aims.gov.au/ereefs-aims/gbr1/dhw_heatstress).

5.4 Validation of DHW products with bleaching observations:

While the snapshot DHW products presented in this report have the same risk category limits as the Coral Reef Watch's DHW, the two integrated DHW products need to be calibrated against observations to understand the risk category limits.

It is essential that a validation of the 3D DHW metrics against bleaching observations at depth be performed in the future. In particular, the observations of bleaching during 2016 and 2017 (Cantin et al., 2020) could be used and compared with the DHW_SSTAARS product.

REFERENCES

Australian Bureau of Meteorology Special Climate Statement 69— an extended period of heavy rainfall and flooding in tropical Queensland. Updated 8 March 2019.

http://www.bom.gov.au/climate/current/statements/scs69.pdf accessed at 10/11/2020.

Baird, A. H., Madin, J. S., Álvarez-Noriega, M., Fontoura, L., Kerry, J. T., Kuo, C.-Y., et al. (2018). A decline in bleaching suggests that depth can provide a refuge from global warming in most coral taxa. Marine Ecology Progress Series 603, 257–264. doi:10.3354/meps12732.

Baker, A. C., Glynn, P. W. & Riegl, B. (2008) Climate change and coral reef bleaching: An ecological assessment of long-term impacts, recovery trends and future outlook. Estuar. Coast. Shelf Sci. 80, 435–471.

Beaman, R.J. 2017. High-resolution depth model for the Great Barrier Reef - 30 m. Geoscience Australia, Canberra. http://dx.doi.org/10.4225/25/5a207b36022d2

Benthuysen, J. A., Oliver, E. C. J., Feng, M., & Marshall, A. G. (2018). Extreme marine warming across tropical Australia during austral summer 2015–2016. Journal of Geophysical Research: Oceans, 123, 1301– 1326. https://doi.org/10.1002/2017JC013326

Benthuysen, J. A., Tonin, H., Brinkman, R., Herzfeld, M., & Steinberg, C. (2016). Intrusive upwelling in the Central Great Barrier Reef. Journal of Geophysical Research: Oceans, 121, 8395– 8416. https://doi.org/10.1002/2016JC012294

Berkelmans, R. & Willis, B. L. (1999) Seasonal and local spatial patterns in the upper thermal limits of corals on the inshore Central Great Barrier Reef. Coral Reefs 18, 219–228

Beyer, HL, Kennedy, EV, Beger, M, et al. (2018) Risk-sensitive planning for conserving coral reefs under rapid climate change. Conservation Letters. 11:e12587. https://doi.org/10.1111/conl.12587

Bridge, T. C. L. et al. (2014). Depth-dependent mortality of reef corals following a severe bleaching event: implications for thermal refuges and population recovery. F1000Research 1–15, https://doi.org/10.12688/f1000research.2-187.v3.

Cantin, N. E., Klein-Salas, E., Frade, P. (2020) Spatial variability in coral bleaching severity and mortality during the 2016 & 2017 GBR coral bleaching event. Report to the National Environmental Science Program. Reef and Rainforest Research Centre Limited, Cairns (54pp.).

Carrigan, A. D. & Puotinen, M. (2014). Tropical cyclone cooling combats region-wide coral bleaching. *Glob. Change Biol.* **20**, 1604–1613 (2014)

DeCarlo T, Harrison HB. (2019). An enigmatic decoupling between heat stress and coral bleaching on the Great Barrier Reef. PeerJ 7:e7473

Donner, S. D. (2011). An evaluation of the effect of recent temperature variability on the prediction of coral bleaching events. Ecol. Appl. 21, 1718–1730.

Donner, S. D. Coping with commitment: Projected thermal stress on coral reefs under different future scenarios. PLoS One 4, (2009).

Eakin, C. M. et al. (2010). Caribbean Corals in Crisis: Record Thermal Stress, Bleaching, and Mortality in 2005. PLoS One 5, e13969

Eakin CM, Liu G, Gomez AM, De la Couri JL, Heron SF, Skirving WJ, Geiger EF, Marsh BL, Tirak KV, Strong AE (2018) Unprecedented three years of global coral bleaching 2014-17. Sidebar 3.1. In: Society BotAM (ed) State of the Climate in 2017

Ebert, E. E. (2009). Neighborhood verification: A strategy for rewarding close forecasts. Weather and Forecasting 24, 1498–1510.

Feng, M., Meyeres, G., Pearce, A. & Wijffels, S. (2003). Annual and interannual variations of the Leeuwin Current at 32°S. *J. Geophys. Res.* **108**, 2156–2202

Fiedler, E. K., McLaren, A., Banzon, V., Brasnett, B., Ishizaki, S., Kennedy, J., et al. (2019). Intercomparison of long-term sea surface temperature analyses using the GHRSST Multi-Product Ensemble (GMPE) system. Remote Sensing of Environment 222, 18–33. doi:10.1016/j.rse.2018.12.015.

Fitt, W. K., Brown, B. E., Warner, M. E., and Dunne, R. P. (2001). Coral bleaching: interpretation of thermal tolerance limits and thermal thresholds in tropical corals. Coral reefs 20, 51–65.

Frade, P. R. et al. Deep reefs of the Great Barrier Reef offer limited thermal refuge during mass coral bleaching. Nat. Commun. 9, 1–8 (2018).

Glynn, P. W. (1996) Coral reef bleaching: facts, hypotheses and implications. Glob. Chang. Biol. 2, 495–509.

Glynn, P. W. & D'Croz, L. (1990). Experimental evidence for high temperature stress as the cause of El Niño-coincident coral mortality. Coral Reefs 8, 181–191.

Green, R.H., Lowe, R.J., Buckley, M.L. *et al.* (2019) Physical mechanisms influencing localized patterns of temperature variability and coral bleaching within a system of reef atolls. *Coral Reefs* **38,** 759–771. https://doi.org/10.1007/s00338-019-01771-2

Heidemann Hanna, Ribbe Joachim, (2019). Marine Heat Waves and the Influence of El Niño off Southeast Queensland, Australia. Frontiers in Marine Science 6, 56, 0.3389/fmars.2019.00056

Heron SF, Eakin CM, Douvere F, Anderson KD, Day JC, Geiger E, Hoegh-Guldberg O, van Hooidonk R, Hughes TP, Marshall P, Obura D (2017) Impacts of Climate Change on World Heritage Coral Reefs: A First Global Scientific Assessment. . UNESCO World Heritage Centre:12

Heron SF, Liu G., Eakin CM, Skirving WJ, Muller-Karger FE, Vega-Rodriguez M, De La Cour JL, Burgess TFR,Strong AE, Geiger EF, Guild LS, Lynds S, (2015). Climatology development for NOAA Coral Reef Watch's 5-km product suite. NOAA technical reports NESDIS 145. Doi:10.7289/V59C6VBS. http://www.star.nesdis.noaa.gov/star/socd_pub.php

Herzfeld, M., J. Andrewartha, M. Baird, R. Brinkman,M. Furnas, P. Gillibrand,M. Hemer, K. Joehnk, E. Jones, D. McKinnon, N. Margvelashvili,M. Mongin, P. Oke, F. Rizwi, B. Robson, S. Seaton, J. Skerratt, H. Tonin, K. Wild-Allen (2016). eReefs Marine Modelling: Final Report, Jan. 2016, CSIRO, Hobart, 497pp.

Hoegh-Guldberg, O. (1999) Climate change, coral bleaching and the future of the world's coral reefs. Mar. Freshw. Res. 50, 839–866

Hughes T. P., Kerry J. T., Álvarez-Noriega M, Álvarez-Romero J. G., Anderson K. D., Baird A. H., Babcock R. C., Beger M., Bellwood D. R., Berkelmans R., Bridge T. C., Butler I. R., Byrne M., Cantin N. E., Comeau S., Connolly S. R., Cumming G. S., Dalton S. J., Diaz-Pulido G., Eakin C. M., Figueira W. F., Gilmour J. P., Harrison H. B., Heron S. F., Hoey A. S., Hobbs J-P. A., Hoogenboom M. O. , Kennedy E. V., Kuo C-y., Lough J. M., Lowe R. J., Liu G., McCulloch M. T., Malcolm H. A., McWilliam M. J., Pandolfi J. M., Pears R. J., Pratchett M. S., Schoepf V., Simpson T., Skirving W. J., Sommer B., Torda G., Wachenfeld D. R., Willis B. L., Wilson S. K. (2017) Global warming and recurrent mass bleaching of corals. Nature 543:373-377

Hughes, T.P., J.T. Kerry, A.H. Baird, S.R. Connolly, A. Dietzel, C.M. Eakin, M.J. McWilliam. (2018) Global warming transforms coral reef assemblages. Nature (2018), p. 1

IPCC (2019) IPCC 2019: Summary for Policymakers Special report on the ocean and cryosphere in a changing climate

Jones RJ (2008) Coral bleaching, bleaching-induced mortality, and the adaptive significance of the bleaching response. Marine Biology 154:65-80

Kessler, W. S., and S. Cravatte (2013). ENSO and short-term variability of the South Equatorial Current entering the Coral Sea, J. Phys. Oceanogr., 43, 956–969, doi:10.1175/JPO-D-12–0113.1.

Langlais, C. E., Lenton, A., Heron, S. F., Evenhuis, C., Sen Gupta, A., Brown, J. N., et al. (2017). Coral bleaching pathways under the control of regional temperature variability. Nature Climate Change 7, 839–844. doi:10.1038/nclimate3399.

Leahy, S. M., Kingsford, M. J. & Steinberg, C. R. (2013). Do clouds save the great barrier reef? Satellite imagery elucidates the cloud-SST relationship at the local scale. *PLoS One* **8**, e70400 (2013)

Liu, G. et al. (2014) NOAA Coral Reef Watch' s Next -Generation 5 km Satellite Coral Bleaching Thermal Stress Monitoring. 29, 27–29.

Liu, G., Strong, A. E. & Skirving, W. (2003) Remote sensing of sea surface temperatures during 2002 Barrier Reef coral bleaching. Eos, Trans. Am. Geophys. Union 84, 137.

Lough, J. M. (1999). Sea surface temperatures on the Great Barrier Reef: A contribution to the study of coral bleaching (Res. Publ. 57). Townsville, QLD: Great Barrier Reef Marine Park Authority. http://hdl.handle.net/11017/331

Marshall, A. T. & Code, P. (2004) Calcification rate and the effect of temperature in a zooxanthellate and an azooxanthellate scleractinian reef coral. 218–224. doi:10.1007/s00338-004-0369-y

McLeod, E., Shaver, E.C., Beger, M., Koss, J., Grimsditch, G. (2021), Using resilience assessments to inform the management and conservation of coral reef ecosystems, Journal of Environmental Management, Volume 277 https://doi.org/10.1016/j.jenvman.2020.111384.

Redondo-Rodriguez Ana, Weeks Scarla J., Berkelmans Ray, Hoegh-Guldberg Ove, Lough Janice M. (2011) Climate variability of the Great Barrier Reef in relation to the tropical Pacific and El Niño-Southern Oscillation. *Marine and Freshwater Research* **63**, 34-47.

Ridgway, K. R., Dunn, J. R., & Wilkin, J. L. (2002). Ocean interpolation by four-dimensional weighted least squares—Application to the waters around Australasia. Journal of atmospheric and oceanic technology, 19(9), 1357-1375.

Roelfsema, C.M., Kovacs, E.M., Ortiz, J.C. et al. (2020) Habitat maps to enhance monitoring and management of the Great Barrier Reef. Coral Reefs 39, 1039–1054. https://doi.org/10.1007/s00338-020-01929-3

Schiller, A., K. R. Ridgway, C. R. Steinberg, and P. R. Oke (2009), Dynamics of three anomalous SST events in the Coral Sea, *Geophys. Res. Lett.*, 36, L06606, doi:10.1029/2008GL036997.

Skirving, W; Marsh, B; De La Cour, J; Liu, G; Harris, A; Maturi, E; Geiger, E; Eakin, CM. CoralTemp and the Coral Reef Watch Coral Bleaching Heat Stress Product Suite Version 3.1. Remote Sens. 2020, 12, 3856; https://doi.org/10.3390/rs12233856.

Smith, T. B. et al. (2016) Caribbean mesophotic coral ecosystems are unlikely climate change refugia. Glob. Chang. Biol. 22, 2756–2765.

Steven, A. D. L., Baird, M. E., Brinkman, R., Car, N. J., Cox, S. J., Herzfeld, M., Hodge, J., Jones, E., King, E., Margvelashvili, N., Robillot, C., Robson, B., Schroeder, T., Skerratt, J., Tickell, S., Tuteja, N., Wild-Allen, K., Yu J., (2019) eReefs: An operational information system for managing the Great Barrier Reef, Journal of Operational Oceanography, 12:sup2, S12-S28, DOI:10.1080/1755876X.2019.1650589

Storlazzi, C.D., Cheriton, O.M., van Hooidonk, R. et al. (2020) Internal tides can provide thermal refugia that will buffer some coral reefs from future global warming. Sci Rep 10, 13435. https://doi.org/10.1038/s41598-020-70372-9

van Hooidonk, R., Maynard, J. a. & Planes, S. (2013) Temporary refugia for coral reefs in a warming world. Nat. Clim. Chang. 3, 508–511.

Venegas, R.M., Oliver, T., Liu, G. et al. (2019) The Rarity of Depth Refugia from Coral Bleaching Heat Stress in the Western and Central Pacific Islands. Sci Rep 9, 19710. https://doi.org/10.1038/s41598-019-56232-1

West, J. M. & Salm, R. V. (2003) Resistance and resilience to coral bleaching: implications for coral reef conservation and management. *Conserv. Biol.* **17**, 956–967

Wijffels, S.E., Beggs, H., Griffin, C., Middleton, J. F., Cahill, M., King, E., Jones, E., Feng, M., Benthuysen, J. A., Steinberg, C. R., & Sutton, P. (2018) A fine spatial-scale sea surface temperature 1 atlas of the Australian regional seas (SSTAARS): seasonal variability and trends around Australasia and New Zealand revisited. Journal of Marine Systems. 187, 156-196

Willmott, C. J. (1981). On the validation of models. Physical Geography, 2, 184–194

Willmott, C. J., Robeson, S. M., and Matsuura, K. (2012). A refined index of model performance. International Journal of Climatology 32, 2088–2094. doi:10.1002/joc.2419.

Zambrano-Bigiarini, M. (2020) hydroGOF: Goodness-of-fit functions for comparison of simulated and observed hydrological time series. R package version 0.4-0. URL https://github.com/hzambran/hydroGOF. DOI:10.5281/zenodo.839854.

APPENDIX 1: DETAILED STATISTICS OF GBR1 VALIDATION

Table A1.1: Code definitions for in situ observations for moorings

Mooring Location	Site Code	Depth (m)	Status	Span
Yongala NRS	NRSYON	30	Current	November 2007 - Present
Darwin NRS	NRSDAR	25	Current	August 2009 - Present
Lizard Slope	GBRLSL	350	Current	October 2007 - May 2014. November 2019 - Present
Myrmidon Reef	GBRMYR	200	Current	October 2007 - Present
Palm Passage	GBRPPS	60	Current	October 2007 - Present
Capricorn Channel	GBRCCH	100	Current	September 2007 - Present
Heron Island South	GBRHIS	45	Current	September 2007 - Present
One Tree East	GBROTE	60	Current	September 2007 - Present

Table A1.2: Summary statistics from the comparison between in situ observations from mooring temperature loggers and the eReefs 1km model. Note the moorings have temperature loggers through the water column and column 2 provides the depth in metres.

SITE	DEPTH	n	TempMean logger	TempMean GBR	Diff. Mean	Diff. Median	Diff. Min.	Diff. Max.	Willmott Mean	pBias Mean	Nrmse mean	Mse mean	CC. mean
GBRCCH	20	1	26.32	26.37	-0.05	0.01	-0.05	-0.05	0.99	0.2	19.4	0.14	0.99
GBRCCH	30	1	26.21	25.90	0.31	0.38	0.31	0.31	0.98	-1.2	28.6	0.31	0.97
GBRCCH	40	1	25.67	25.26	0.41	0.30	0.41	0.41	0.94	-1.6	43.1	0.80	0.93
GBRCCH	50	1	25.53	24.94	0.59	0.36	0.59	0.59	0.89	-2.3	56.6	1.41	0.88
GBRCCH	60	1	25.71	24.56	1.15	1.20	1.15	1.15	0.82	-4.5	76.6	2.60	0.86
GBRCCH	70	1	25.36	24.35	1.01	0.98	1.01	1.01	0.83	-4.0	74.0	2.28	0.85
GBRCCH	80	1	24.92	24.50	0.42	0.34	0.42	0.42	0.96	-1.7	36.9	0.70	0.97
GBRHIS	10	1	25.54	25.66	-0.12	-0.14	-0.12	-0.12	0.99	0.5	15.4	0.07	0.99
GBRHIS	15	1	25.04	25.29	-0.24	-0.19	-0.24	-0.24	0.99	1.0	19.5	0.17	0.99
GBRHIS	20	1	24.89	25.17	-0.28	-0.22	-0.28	-0.28	0.99	1.1	20.3	0.20	0.99
GBRHIS	25	1	24.85	25.17	-0.31	-0.24	-0.31	-0.31	0.99	1.3	21.8	0.23	0.99
GBRHIS	30	1	22.55	22.87	-0.32	-0.32	-0.32	-0.32	0.98	1.4	26.3	0.18	0.98
GBRMYR	10	1	27.40	27.57	-0.17	-0.19	-0.17	-0.17	0.99	0.6	20.1	0.12	0.99
GBRMYR	20	1	27.24	27.09	0.14	0.15	0.14	0.14	0.98	-0.5	26.3	0.17	0.97

SITE	DEPTH	n	TempMean logger	TempMean GBR	Diff. Mean	Diff. Median	Diff. Min.	Diff. Max.	Willmott Mean	pBias Mean	Nrmse mean	Mse mean	CC. mean
GBRMYR	30	1	27.36	26.97	0.39	0.34	0.39	0.39	0.95	-1.4	43.6	0.45	0.93
GBRMYR	40	1	27.16	26.65	0.52	0.42	0.52	0.52	0.91	-1.9	57.6	0.70	0.89
GBRMYR	50	1	26.89	26.30	0.59	0.47	0.59	0.59	0.87	-2.2	68.9	0.86	0.85
GBRMYR	60	1	26.58	25.92	0.66	0.53	0.66	0.66	0.83	-2.5	80.1	1.02	0.80
GBRMYR	70	1	26.26	25.46	0.80	0.69	0.80	0.80	0.78	-3.0	94.3	1.23	0.77
GBRMYR	80	1	25.92	24.93	0.99	0.92	0.99	0.99	0.72	-3.8	113.5	1.62	0.73
GBRMYR	90	1	25.47	24.36	1.11	1.09	1.11	1.11	0.67	-4.4	125.9	1.85	0.73
GBRMYR	100	1	24.94	23.73	1.21	1.18	1.21	1.21	0.64	-4.9	132.6	2.11	0.71
GBRMYR	110	1	24.36	23.06	1.30	1.29	1.30	1.30	0.60	-5.3	148.1	2.31	0.68
GBRMYR	120	1	23.66	22.38	1.28	1.29	1.28	1.28	0.60	-5.4	149.4	2.33	0.65
GBRMYR	130	1	22.92	21.72	1.20	1.26	1.20	1.20	0.61	-5.2	134.0	2.31	0.60
GBRMYR	140	1	22.13	21.06	1.07	1.14	1.07	1.07	0.62	-4.8	117.7	2.27	0.57
GBRMYR	150	1	21.30	20.54	0.76	0.82	0.76	0.76	0.63	-3.6	104.1	1.84	0.52
GBRMYR	160	1	20.51	20.02	0.49	0.51	0.49	0.49	0.62	-2.4	99.2	1.60	0.45
GBRMYR	170	1	19.81	19.58	0.23	0.22	0.23	0.23	0.60	-1.2	99.0	1.41	0.37
GBRMYR	180	1	19.20	19.20	-0.01	0.00	-0.01	-0.01	0.54	0.0	103.6	1.37	0.28
GBRMYR	190	1	18.61	18.83	-0.22	-0.21	-0.22	-0.22	0.49	1.2	112.0	1.38	0.20
GBROTE	20	1	24.99	24.68	0.32	0.35	0.32	0.32	0.96	-1.3	34.2	0.47	0.96
GBROTE	25	1	24.86	24.65	0.21	0.26	0.21	0.21	0.97	-0.9	31.9	0.40	0.96
GBROTE	30	1	24.72	24.59	0.14	0.17	0.14	0.14	0.97	-0.6	31.3	0.38	0.96
GBROTE	35	1	24.59	24.46	0.13	0.15	0.13	0.13	0.97	-0.5	33.2	0.42	0.96
GBROTE	40	1	24.43	24.32	0.11	0.11	0.11	0.11	0.96	-0.5	36.4	0.50	0.94
GBROTE	45	1	24.01	24.08	-0.07	-0.08	-0.07	-0.07	0.96	0.3	34.6	0.47	0.95
GBROTE	50	1	23.81	24.01	-0.21	-0.21	-0.21	-0.21	0.96	0.9	38.1	0.55	0.94
GBROTE	55	1	22.78	23.37	-0.59	-0.56	-0.59	-0.59	0.91	2.6	57.3	0.87	0.90
GBRPPS	20	1	27.30	27.25	0.05	0.07	0.05	0.05	0.98	-0.2	28.1	0.21	0.96
GBRPPS	30	1	27.49	27.29	0.21	0.17	0.21	0.21	0.95	-0.8	43.1	0.44	0.91
GBRPPS	40	1	26.58	26.28	0.30	0.20	0.30	0.30	0.93	-1.1	49.4	0.63	0.89
GBRPPS	50	1	26.14	25.76	0.38	0.23	0.38	0.38	0.90	-1.4	57.7	0.88	0.85
GBRPPS	60	1	25.56	25.21	0.35	0.19	0.35	0.35	0.90	-1.4	56.9	0.87	0.85
NRSYON	10	1	25.93	26.31	-0.38	-0.43	-0.38	-0.38	0.98	1.5	25.4	0.27	0.99
NRSYON	20	1	25.84	26.13	-0.29	-0.36	-0.29	-0.29	0.99	1.1	24.1	0.24	0.98
NRSYON	30	1	25.83	26.18	-0.35	-0.35	-0.35	-0.35	0.99	1.4	22.6	0.21	0.99

Table A1.3: Summary statistics from the comparison between in situ observations from all of the reef temperature loggers aggregated here for validation and the eReefs 1km model. Note the temperature loggers are deployed at different depths and are grouped according to their generic reef location (Channel – CH; Reef Flat – FL, Reef Slope – SL). Column 2 provides the depth in metres referenced to Lowest Astronomical Tide (LAT) and Column 3 indicates the number used in this comparison for each reef location and depth.

Location ID	DEPTH	# Locations	TempMean logger	TempMean GBR	Diff. Mean	Diff. Median	Diff. Min.	Diff. Max.	Diff. sd	Willmott Mean	pBias Mean	Nrmse mean	Mse mean	CC. mean
CH	2	5	27.56	28.16	-0.60	-0.66	-0.83	-0.30	0.26	0.77	2.18	128.88	0.59	0.86
CH	3	4	28.10	28.89	-0.79	-0.73	-0.86	-0.73	0.06	0.59	2.85	175.65	0.88	0.69
CH	6	4	27.07	27.50	-0.43	-0.38	-0.73	-0.21	0.23	0.86	1.60	77.83	0.34	0.91
CH	9	3	27.84	28.10	-0.26	-0.17	-0.42	-0.17	0.14	0.84	0.90	68.57	0.23	0.81
CH	10	1	26.85	26.90	-0.06	0.08	-0.06	-0.06	-	0.97	0.20	34.10	0.58	0.94
FL	1	2	25.11	25.34	-0.23	-0.28	-0.25	-0.20	0.03	0.76	0.90	62.50	0.62	0.70
FL	2	85	26.70	27.02	-0.31	-0.27	-1.28	0.55	0.38	0.94	1.21	40.44	0.63	0.94
FL	3	8	27.74	28.26	-0.52	-0.42	-1.15	-0.12	0.39	0.87	1.86	76.50	0.59	0.92
FL	4	11	26.38	26.95	-0.57	-0.45	-1.66	-0.14	0.44	0.94	2.15	38.56	0.91	0.93
FL	5	1	26.86	27.44	-0.58	-0.58	-0.58	-0.58	-	0.98	2.20	26.20	0.49	0.99
SL	2	1	25.63	26.40	-0.77	-0.79	-0.77	-0.77	-	0.96	3.00	39.60	0.69	0.99
SL	4	1	28.59	28.37	0.22	0.18	0.22	0.22	-	0.99	-0.80	24.40	0.16	0.98
SL	5	21	26.97	27.44	-0.47	-0.47	-0.92	-0.03	0.26	0.93	1.79	48.83	0.47	0.97
SL	6	56	26.65	26.80	-0.15	-0.16	-0.71	0.66	0.29	0.96	0.58	36.04	0.28	0.96
SL	7	9	26.58	26.86	-0.27	-0.27	-0.69	0.01	0.23	0.88	1.02	72.48	0.31	0.86
SL	8	12	26.92	27.20	-0.28	-0.16	-0.90	0.16	0.34	0.90	1.01	64.50	0.32	0.96
SL	9	7	27.12	27.34	-0.22	-0.17	-0.64	0.01	0.21	0.98	0.81	27.49	0.27	0.98
SL	10	5	26.02	26.29	-0.27	-0.25	-0.46	-0.17	0.12	0.98	1.04	27.22	0.25	0.98

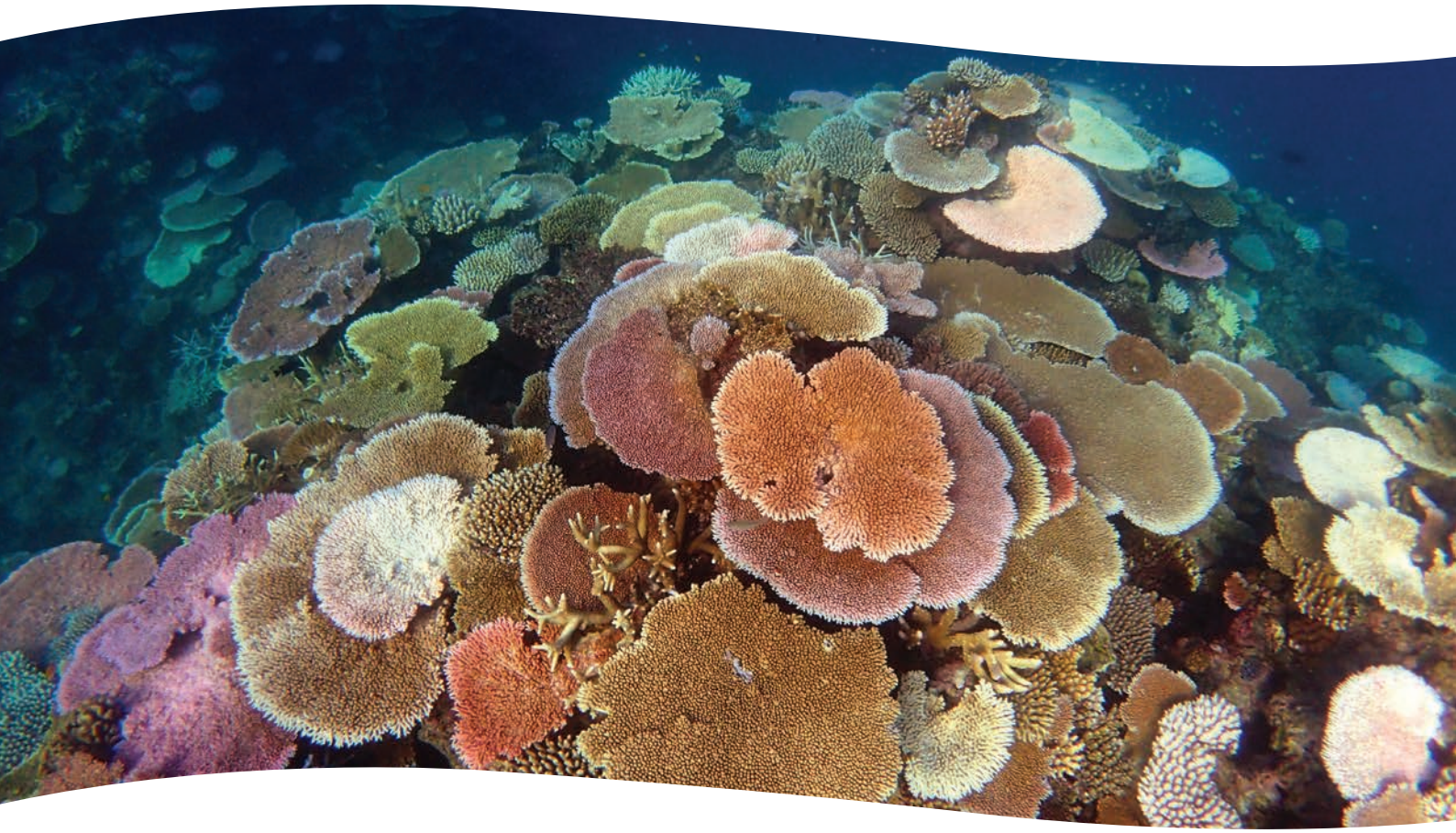

Reef & Rainforest
RESEARCH CENTRE

www.nesptropical.edu.au